28

Uncertainty of the PMP and PMF

Jose D. Salas
Colorado State University

Germán Gavilán
University of California, Merced

Fernando R. Salas
The University of Texas at Austin

Pierre Y. Julien
Colorado State University

Jazuri Abdullah
Colorado State University

AUTHORS

Jose D. Salas is a professor emeritus of civil and environmental engineering at Colorado State University (CSU). He received BS and civil engineering degrees from the National University of Engineering of Lima, Perú; MSc degree in hydraulics; and PhD degree in hydrology and water resources from CSU. At CSU, he supervised (main advisor) 42 MSc and 37 PhD students. Dr. Salas has been consultant of national and international organizations and worked in several countries sponsored by UNESCO, FAO, AID, IICA, Hydro-Quebec, and the World Bank. Dr. Salas has been member of the editorial board of several international journals and has published extensively in water resources literature including two books and 12 chapters in books and handbooks. He was awarded the 1996 Arid Lands Hydraulic Engineering Award and the 2010 Ven Te Chow Award both by the American Society of Civil Engineers. He is a corresponding member of the Academy of Engineering of Mexico and the Academy of Engineering of Peru.

Germán Gavilán is an assistant dean of engineering at the University of California at Merced (UC Merced) and chief scientist at the Center for Information Technology Research in the Interest of Society (CITRIS). He received a bachelor degree in civil engineering from Universidad Industrial de Santander (UIS) in Colombia, MSc degree in water resources, and PhD degree in environmental engineering from Purdue University. Prior to joining UC Merced, he was professor at the School of Civil Engineering and Environmental Engineering at UIS, where he was also head of the Civil Engineering School for three years

and chair of the water resources graduate program for two years. He has been a consultant in the areas of water resources, hydrology, and environmental engineering for various private and government agencies for over 25 years. He is the author or coauthor of four books in the fields of hydraulics and hydrology.

Fernando R. Salas is a PhD student in environmental and water resources engineering at the University of Texas at Austin where he received his MSE degree in 2010. Through the Center for Research in Water Resources (CRWR) at the University of Texas, Mr. Salas has focused his research on the development of environmental information systems that improve the knowledge and understanding of the water cycle. Since 2010, Mr. Salas has been an active member of the Greater Austin Chapter of Engineers without Borders where he has worked on projects in Panama and Peru. He is currently the founder and co-project lead of the Climate Adaptation in Mountain Basins in the Andean Region (CAMBIAR) program. Before moving to Texas, Mr. Salas received his BS in civil and environmental engineering from Cornell University in 2008.

Pierre Y. Julien is a professor of civil and environmental engineering at CSU. He received BSc degree in civil engineering, MSc degree in hydraulics, and PhD degree in hydraulics from Laval University, Canada. His research interest includes river mechanics, hydraulics, and hydrologic modeling. At CSU, he supported and guided 58 MSc and 33 PhD students. Dr. Julien has been consultant of national and international organizations and worked in several projects in various countries such as India, Malaysia, Peru, Korea, and Canada. He was editor of the *ASCE Journal of Hydraulic Engineering* during 2002–2005 and received several awards including the H. A. Einstein Award from the American Society of Civil Engineers. Dr. Julien has published extensively in water resources literature including two books and 20 lecture manuals and book chapters.

Jazuri Abdullah is a PhD student in civil and environmental engineering at CSU. He received bachelor of engineering degree from the University of Technology, MARA (UiTM), Malaysia and the MSc degree in water resources engineering and management from the University of Stuttgart, Germany. Mr. Abdullah is also a lecturer of the Faculty of Engineering at UiTM and is a member of the Board of Engineers of Malaysia (BEM) and a graduate member of the Institute of Engineers of Malaysia (IEM).

PREFACE

Probable maximum precipitation (PMP) and probable maximum flood (PMF) have been commonly used in engineering practice for designing major hydraulic structures. However, in recent decades, there has been a growing concern regarding the uncertainties involved in estimating such extreme events. In this chapter, the concepts and methods for estimating the PMP and PMF considering their associated uncertainties are examined. After briefly reviewing the underlying concepts and definitions, an overview of the methods for estimating the PMP is presented, which includes hydrometeorological methods, the statistical method by Hershfield, and some other statistical alternatives. Regardless of the methods applied for obtaining the PMP and PMF, a number of studies have shown that their estimates involve many uncertainties. While hydrometeorological methods likely provide the best estimates of PMP, however, in many regions of the world, hydrometeorological data are lacking, and consequently feasibility studies and designs of flood-related projects are being made based solely on Hershfield's statistical method that provides a single value for the PMP. Thus, a method for quantifying the uncertainty of the PMP if Hershfield's method is to be applied has been included in this chapter. Furthermore, the chapter includes sensitivity analysis, Monte Carlo analysis, and some statistical alternatives for PMF estimation and uncertainty.

28.1 Introduction

Probable maximum precipitation (PMP) and the corresponding probable maximum flood (PMF) have commonly been utilized in engineering practice [81], particularly for designing hydraulic structures such as spillways of large dams whose failure may cause losses of life and catastrophic damage to nuclear power plants. In the United States, many federal and state agencies use the PMP and PMF for evaluating the adequacy and safety of major hydraulic structures. Regardless of the method utilized for obtaining the PMP, the practice of designing and evaluating flood-related structures based on such PMP has been criticized among others because of the many uncertainties involved in determining them, the lack of a standard approach for estimating the PMP, and the perception that such estimated PMP (and the ensuing PMF) is an upper bound that may not be exceeded and as such a zero risk. However, an upper bound with zero risk is not realistic because there have been documented cases where the recorded floods have exceeded the estimated PMFs [4,15,45]. Thus, a risk-based design approach has been advocated by some hydrologists. For instance, Dawdy and Lettenmaier [15] suggested as an alternative "to retain the PMF as a reference event and estimate its exceedance probability." And they added "…there will be uncertainties associated with any risk estimates, especially for flood peaks and volumes with exceedance probabilities as low as those for the PMF. Any rational design approach must recognize this uncertainty."

Therefore, in this chapter, the concepts and methods for estimating the PMP and PMF considering their associated uncertainties are examined. The main purpose is to summarize the alternative methods that are available for determining the uncertainties involved in estimating the PMP and PMF. The second section is a brief review of concepts and definitions of the PMP and PMF. The third section gives an overview of the classical methods for estimating the PMP such as hydrometeorological methods, the statistical method by Hershfield, and some other statistical alternatives. The fourth section discusses the uncertainty of the PMP considering hydrometeorological factors, and Section 28.5 presents in some detail a procedure for estimating the uncertainty of the PMP based on Hershfield's method. Section 28.6 describes PMF estimation and uncertainty, which includes sensitivity analysis and Monte Carlo analysis, as well as some statistical alternatives. The chapter ends with a section of concluding remarks.

28.2 Concepts and Definitions of the PMP and PMF

PMP has its origin in what used to be called maximum possible precipitation (MPP) where it was defined as an upper bound maximum value [4], that is, the concept was to find a maximum value of precipitation for a given storm duration over a basin that physically could occur but would not be exceeded. Unfortunately, it has been reported in literature that in some real cases, such MPP values have been exceeded [4]. This observation as a consequence has led to the renaming of "maximum possible precipitation" to "PMP." Thus, the PMP definition that has been widely accepted in literature is: "theoretically the greatest depth of precipitation for a given storm duration that is physically possible over a given size storm area at a particular geographical location at a certain time of the year" [31,83]. The PMP definition used by the World Meteorological Organization (WMO) [84] has been slightly changed, but the essence remains the same. The referred definition highlights the PMP as a physical upper limit, and often it is perceived to be a quantity that cannot be exceeded. However, WMO [84] acknowledges the fact that the value of the PMP that is calculated for a particular study area is only an approximation "due to the physical complexity of the phenomena and limitations in data and the meteorological and hydrological sciences." Furthermore, as hinted by WMO [83], one must distinguish between the "theoretical PMP," that is, an upper limit that is unknown, and the "operational PMP," which is the PMP obtained by a given method that involves a number of assumptions, steps, and data that are uncertain.

The PMF is a deterministic upper limit flood that is commonly utilized as a design criterion by several organizations in many countries. However, the PMF is not so generally defined as the PMP. Newton [55] cites various definitions used by different US and international agencies. The PMF definition used

by some organizations such as the US Bureau of Reclamation (USBR) is "the maximum runoff condition resulting from the most severe combination of hydrologic and meteorological conditions that are considered reasonably possible for the drainage basin under study" [14]. Other similar definitions of PMF are: "a flood that can be expected from the most severe combination of critical meteorologic and hydrologic conditions that are reasonably possible in a region" [34] and "PMF is the theoretical maximum flood that poses extremely serious threat to the flood control of a given project in a design watershed. Such a flood could plausibly occur in a locality at a particular time of the year under current meteorological conditions" [84]. The PMF is generally viewed as the flood resulting from a PMP, plus snowmelt where appropriate, applied to assumed antecedent basin conditions. However, the assumptions and procedures for selecting antecedent conditions and estimating the flood hydrograph from the PMP vary depending on the country, agency, and hydrologist. For example, there are some aspects of the PMP to PMF conversion that are unique to the USBR [73].

28.3 Overview of Methods for Estimating the PMP

The manual of WMO [84] describes six methods for estimating the PMP: (a) the local method (local storm maximization model), (b) the transposition method (storm transposition model), (c) the combination method (temporal and spatial maximization of storm), (d) the inferential method (theoretical model), (e) the generalized method, and (f) the statistical method. In addition, the manual describes two other methods that may be applicable for very large basins. The previous methods, categorized as hydrometerological (a–e) are generally based on deterministic approaches, that is, based on physical laws and principles, while method (f) is essentially the statistical method proposed by Hershfield [35,36]. The previous methods, categorized as hydrometeorological methods, the statistical method by Hershfield, and some statistical alternatives (that have been proposed in the last three decades), are summarized in the following section.

28.3.1 PMP Based on Hydrometeorological Methods

There are several key references in literature outlining in some detail the various hydrometeorological methods available for estimating the PMP [31,32,84]. Modifications and improvements have evolved over the years. Hansen [32] summarized the developments through the mid-1980s for the various regions of the United States and discussed advances in estimating the PMP for regions where the convergence (nonorographic) and orographic components of the PMP can be determined. Hansen also reexamined the data of estimates of PMPs and observed storms obtained by Riedel and Schreiner [69] and concluded that the PMP estimates were not too high. For example, for the east of the 105th meridian, out of 75 storms considered, 18 storms exceeded 70% of the PMPs and three storms exceeded 90%. Recently England et al. [25] reviewed the various PMP procedures and databases used in estimating the PMP based on hydrometeorological methods particularly those utilized for developing the hydrometeorological reports (HMRs) that provide generalized PMP estimates over large regions of the United States (e.g., HMR 58 for California). They also described the key concepts involved including depth-area duration analysis of large storms, storm maximization, storm transposition, and envelopment. Further technical details of the underlying concepts and procedures may be found in Hansen et al. [33] and WMO [84].

The methods based on storm models use physical parameters such as dew point temperature, storm depth, and inflow and outflow fluxes depending on the storm type [12]. For example, in areas subject to the occurrence of hurricanes, a hurricane model may be applied for estimating the PMP. An advection–diffusion model of clouds for determining the temporal and spatial dynamics of extreme precipitation in a catchment located in the Bernese Alps of Switzerland has been suggested [67]. Atmospheric models such as the Regional Atmospheric Modeling System (RAMS) and the fifth-generation NCAR/Penn State mesoscale model (MM5) are being investigated for modeling extreme rainfall [13,62]. Storm maximization consists of adjusting a large observed storm precipitation to enable the convergence of the

maximum atmospheric moisture, that is, moisture maximization is increasing storm rainfall depth for the location and season, for higher atmospheric moisture than was available in the actual storm [25,37]. Transposition of storms means that the observed storm at a given location is translated to another location (say for an ungauged basin area) with appropriate adjustments such as those for differences in altitude [83]. The method assumes a region of homogeneous meteorology and topography. Using probability concepts for storm transposition has been examined by some researchers [1,30,26,27]. The regionalization methods (also called generalized PMP) are developed for large areas and generally are based on maximization and transposition of several types of storms (e.g., convective or cyclonic storms), depth–area–duration analysis, and envelopment. An example of this method is that developed by the National Weather Service of the United States [59]. Applications and developments in several other countries can be found in WMO [84 and the references therein].

28.3.2 PMP Based on Hershfield's Statistical Method

Hershfield's statistical method [35,36] was developed as an alternative to the traditional methods that are based on physical concepts. Hershfield's method, popularized internationally by WMO [82–84], has been commonly utilized in practice, particularly for basins lacking hydrometeorological data. It has been utilized in several countries worldwide for comparing with other methods for determining the PMP [2] and for preliminary and feasibility hydrologic studies [5]. Hershfield's statistical method is based on an equation similar to that of Chow [9] where a quantile of the underlying distribution is expressed as a function of the sample mean, the sample standard deviation, and a frequency factor K [10]. In the typical procedure for fitting the empirical frequency distribution of the data at hand using a probability distribution function (PDF), the value of K is related to the skewness coefficient and the exceedance probability. But in Hershfield's method, the value of K was established after analyzing a large number of historical data of storm annual daily maximums so that an upper bound of K was determined, which was bigger than all values of K obtained from the historical sample.

Hershfield's method was based on 24 h maximum precipitation data of 2645 stations (90% of which were stations in the United States and the rest for other parts of the world), which gave a total of about 95,000 station-year data. The method uses the equation

$$PMP = \bar{X}_n + K S_n \tag{28.1a}$$

where

$\bar{X}_n$ is the mean annual maximum daily precipitation
S_n is the corresponding standard deviation
K is a frequency factor

Hershfield recognized that because $\bar{X}_n$ and S_n are quantities that are estimated from a limited sample (n), they must be adjusted for sample size and for the effect of outliers. Graphs are available for obtaining the appropriate adjustment factors [35,83,84]. Another correction suggested by Hershfield was to account for the difference that exists between the daily maximum values and the 24 h maximums regardless of the calendar day.

Based on the data analysis of the 2,645 sites, Hershfield [35] found that the value of K in (28.1a) varied in the range 1.00–14.99 and that K ranged between 13.00 and 14.49 for only four stations. Consequently, he suggested utilizing the value of $K = 15$ for estimating the PMP. However, additional studies by Hershfield [36] indicated that K varied with the storm duration and the mean annual maximum precipitation; therefore, he provided additional relations (graphs) that enable one in determining the value of K for practical applications. Furthermore, other studies appeared in literature documenting the most appropriate values of K according to the climatic region of the study area. For example, Mejía and Villegas [50] analyzed 1, 2, and 24 h duration storm data for Colombia and suggested the corresponding envelopes for

determining K as a function of the mean annual maximum precipitation. Similar studies can be found for other locations in the world such as the southern half of the Indian peninsula [17], the Alpine region in Austria [56], the north region of India [66], the Czech Republic [68], the south region of Malaysia [16], and the Cataluña region of Spain [8]. Hershfield [35, pp. 101–102] recognized that K is a random variable and illustrated this point by associating the values of K with the return period (or exceeding probability) using as examples the Gumbel and lognormal distributions. Nevertheless, his rationale and intent was finding a value (actually an envelope function) that could be applicable for a given storm duration and climatic region. Such an envelope was obtained based on a large database of numerous storms that have been observed in historical records at similar locations. Hershfield [36, p. 967] argued that "enveloping K as a function of the mean serves a transposition purpose."

For easy of explanation and subsequent reference, Hershfield's method may be summarized as follows: (a) adjust $\bar{X}_n$ and S_n for effect of outlier; (b) adjust $\bar{X}_n$ and S_n for effect of sample size; (c) select K as a function of $\bar{X}_n$, the storm duration, and the study region; (d) estimate the PMP from (28.1a); and (e) make an additional adjustment to account for the difference between the maximum of a given time period (storm duration) and the maximum of the observation time period (e.g., to account for the difference between the maximum of 1440 min storm duration and the maximum observed daily).

28.3.3 Statistical Alternatives for Estimating Extreme Precipitation (Including PMP)

Koutsoyiannis [45] argued that K used by Hershfield could be fitted using some type of PDF and suggested the general extreme value (GEV) as a logical function since it deals with extreme events. Koutsoyiannis reexamined Hershfield's results and concluded that the $K = 15$ suggested by Hershfield corresponds approximately to a return period of 60,000 years based on the GEV distribution. Koutsoyiannis also illustrated his alternative approach using 136 years of data of annual maximum daily rainfall in Greece. As expected, such a long record offers the alternative of fitting the frequency distribution of the data and finding quantiles for any desired return period. Likewise, Papalexiou and Koutsoyiannis [63] suggested finding design values of maximum precipitation simply using the frequency analysis of the observed data based on the GEV distribution. Douglas and Barros [19] approached the design of maximum precipitation using a completely different method, which is based on applying multifractal concepts for determining what they called the fractal maximum precipitation (FMP), and applied their approach to the eastern United States.

In addition to the proposed methods summarized previously, efforts have been made to extend (extrapolate) the traditional frequency curves (FCs) that may be obtained from historical records at single sites. However, extending the FCs also implies increasing uncertainty of the estimated quantiles. Figure 28.1 illustrates the "credible" limits of extrapolation for events considered as large, rare, and extreme as the annual exceedance probability (AEP) increases [53]. A technique that is often used for extrapolating the FCs is based on regional precipitation frequency analysis (e.g., using the index flood approach). This way one can determine precipitation quantiles for return periods further beyond the usual historical record lengths, which may be of the order of 50–100 years. Table 28.1 summarizes the ranges of "credible extrapolation" for various types of data and methods [53,77]. Also, the tendency has been to assign an AEP to the PMP. While assigning an AEP to the PMP may be inconsistent with the "upper limit" concept of the PMP, it has been argued that given that the PMP is an uncertain quantity, it may conceivably be exceeded [53]. Based on a review conducted by Laurenson and Kuczera [47] on studies made in Australia and elsewhere and considering that at present there is no conceptually sound basis for assigning an AEP to the PMP, a recommendation was made where the AEP of PMP estimates vary solely as a function of catchment area [53]. The recommendation is summarized in Figure 28.2. Note that Nathan and Merz [54] cautions that "there is considerable uncertainty surrounding these recommendations as they are for events beyond the realm of experience and are based on methods whose conceptual foundations are unclear."

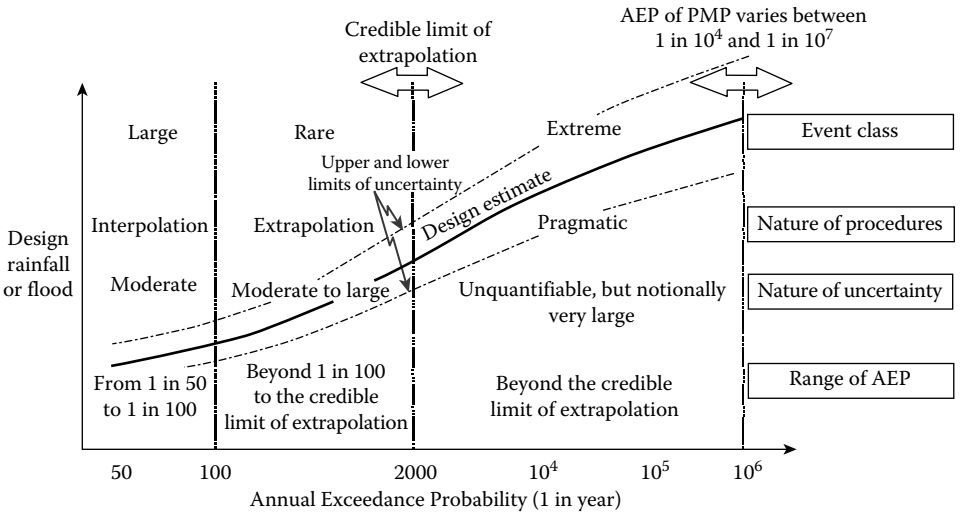

FIGURE 28.1 Increase of design events and corresponding uncertainty as the Annual Exceedance Probability (AEP) increases. (From Nathan, R.J. and Weinmann, P.E., Estimation of large to extreme floods, Book VI, *Australian Rainfall and Runoff: A Guide to Flood Estimation*, National Committee on Water Engineering, Institution of Engineers, Australia, 2001. With permission.)

TABLE 28.1 Data Type and Extrapolation Ranges for Frequency Analysis of Extreme Events

	Range of Credible Extrapolation for AEP	
Type of Data Used for Frequency Analysis	Typical	Most Optimistic
At-site precipitation data	1 in 100	1 in 200
At-site gauged streamflow data[a]	1 in 100	1 in 200
Regional streamflow data[b]	1 in 500	1 in 1,000
At-site streamflow and at-site paleoflood data[c]	1 in 4,000	1 in 10,000
Regional precipitation data	1 in 2,000	1 in 10,000
Regional streamflow and regional paleoflood data	1 in 15,000	1 in 40,000
Combination of regional data sets and extrapolation	1 in 40,000	1 in 100,000
[a]At-site gauged streamflow data (Australia)	1 in 50	1 in 200
[b]At-site/regional gauged streamflow data (Australia)	1 in 200	1 in 500
[c]At-site gauged and paleoflood data (Australia)	1 in 5,000	1 in 10,000

Source: Adapted from Nathan, R.J. and Weinmann, P.E., Estimation of large to extreme floods, Book VI, *Australian Rainfall and Runoff: A Guide to Flood Estimation*, National Committee on Water Engineering, Institution of Engineers, Australia, 2001; US Bureau of Reclamation, A framework for characterizing extreme floods for dam safety risk assessment, prepared by Utah State University and USBR, Denver, CO, 67pp., 1999. With permission.

28.4 Uncertainty of the PMP Considering Hydrometeorological Factors

The most recent manual of the WMO [84] states "Storms, and their associated floods, have physical upper limits, which are referred to as PMP and PMF. It should be noted that due to the physical complexity of the phenomena and limitations in data and the meteorological and hydrological sciences, only approximations

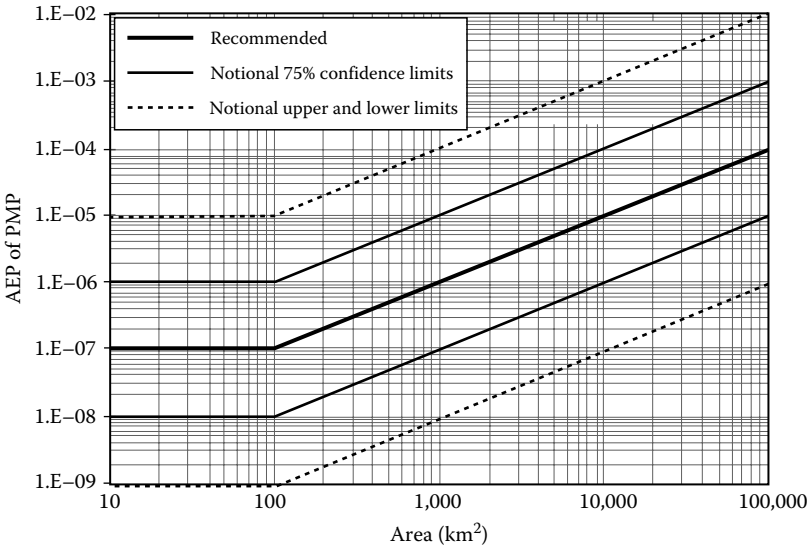

FIGURE 28.2 Values of AEP of PMP as a function of the catchment area. (From Nathan, R.J. and Weinmann, P.E., Estimation of large to extreme floods, Book VI, *Australian Rainfall and Runoff: A Guide to Flood Estimation*, National Committee on Water Engineering, Institution of Engineers, Australia, 2001. With permission.)

are currently available for the upper limits of storms and their associated floods." This concept must be clearly understood by water resources specialists involved in determining the so-called PMP and PMF.

The US National Research Council [58] considers two types of uncertainties that are summarized as follows: (1) Natural uncertainty represents the inherent variability of the physical system; it cannot be reduced. For example, if a given system is represented by a PDF say $f(x,\underline{\theta})$ with known parameter set $\underline{\theta}$, then X is random and as such its variability (uncertainty) is irreducible. (2) Knowledge uncertainty is due to the lack of understanding of the system and insufficient data. Using the same example as previously discussed, suppose we know the PDF but the parameter set $\underline{\theta}$ is unknown, so it must be estimated from data such as $x_1, x_2, \ldots, x_N$ where N is the sample size. Then, the parameter set is now referred to as $\hat{\underline{\theta}}$ and any quantile say $\hat{X}_q$ will be uncertain because of the uncertainty of the parameter set. However, knowledge uncertainty is reducible, for example, as the sample size N increases, the uncertainty of $\hat{\underline{\theta}}$ and consequently the uncertainty of $\hat{X}_q$ will decrease. In fact, as $N \to \infty$, the uncertainty of $\hat{\underline{\theta}}$ (and the uncertainty of $\hat{X}_q$) will become zero. Note that generally the PDF $f(x,\underline{\theta})$ is also unknown. Sometimes knowledge uncertainty has been referred to as "epistemic" [51].

As example of the previous concepts, we illustrate a method for determining the uncertainty of extreme precipitation (approaching the PMP) considering some of the hydrometeorological factors involved in estimating the PMP. Papalexiou and Koutsoyiannis [63] argued that the estimates of the PMP based on maximization of storm moisture do not appear having an upper bound. Based on the analysis of dew point temperature, atmospheric moisture, and maximized precipitation, they concluded that no upper bounds of the PMP estimates were evident. Instead of using the variability of these factors as they affect the estimates of PMP, the concepts proposed by Klemes et al. [43] and Klemes [44] are described. The concepts are simple but have important implications for estimating precipitation FCs for extreme events and near the PMP. Actually two approaches were suggested that are summarized as follows. Let us consider that N years of one-day maximum rainfall data R_t are available for a given site. Based on this data set, one can make frequency analysis following any well-known technique. Let us further assume that it is possible to separate the one-day maximum rainfall R_t into the convergence component C_t and the orographic component O_t. Thus, three sets of data of length N years each would be available. Klemes argued that the occurrence of the

convergence part of the storm is independent of the occurrence of the orographic part since they depend on different physical mechanisms. Then it is possible that in any given year, the maximum one-day rainfall may arise from any combination of the convergence and orographic components. Therefore, the combination of the two sets of data, that is, the convergence and orographic, will produce data of size N^2, which is a significant gain. For example, if $N = 100$, the procedure outlined previously will lead to 10,000 data points.

The second approach suggested by Klemes et al. [43] builds on the same concept as in the previous discussion but brings a third component, that is, moisture maximization of storms and precipitable water (storm efficiency). The assumption is to combine the actual P/M ratio of a given storm (where P and M stand for precipitation and precipitable water, respectively) with the maximum observed precipitable water. Considering the P/M ratios of the orographic and convergence components as independent, the N orographic P/M ratios are combined with the N convergence P/M ratios yielding N^2 total storm P/M ratios that are then combined with the N values of precipitable water. Thus, a total sample of N^3 possible precipitation values are obtained, which can be useful for frequency analysis.

Klemes et al. [43] and Klemes [44] illustrate the previous approaches for estimating the one-day PMP at Coquitlam Lake (CL) basin in Canada. The basin has an area of 193 km^2, is located in the western Coast Mountains (elevations ranging from 153 m to over 2000 m), and is about 30 km NE of Vancouver. The referred authors used 40 years of relevant hydrometeorological variables such as maximum one-day precipitation and precipitable water, that is, $N = 40$. Various estimates of the PMP using the traditional hydrometeorological methods have been made for CL, and the referred papers suggest for comparison a PMP of about 400 mm. Precipitation essentially free of orographic influence is recorded at Vancouver International Airport (the airport is located in the general direction of the southwesterly flows) and has been considered as a good approximation of the convergence component of CL precipitation. Thus, the orographic component was estimated as the difference between the total precipitation recorded at CL and that recorded at the airport. Figure 28.3 shows the precipitation FCs for the total precipitation at CL and those for the two components. Also Figure 28.3 shows with arrows a graphical extrapolation through 100 years (which is about twice the length of record, i.e., $2N$ in general). The resulting FC based on the combined sample of length 1600 (40^2) is shown in Figure 28.4. The figure shows also the original FC based on the original sample of size 40 (square symbol). Figure 28.4 shows a pretty good agreement between the two FCs. Also note the final point (based on the extrapolations in Figure 28.3 as previously indicated), which shows a precipitation of 340 mm corresponding to about 10,000 years of return period. Figure 28.4 also points to about 100,000 years of return period for the estimated PMP of 400 mm. The interested reader may refer to the paper by Klemes et al. [43] for applications using the approach based on storm maximization, which enables one estimating the uncertainty of precipitation further closer to the range of the estimated value of the PMP.

28.5 Uncertainty of the PMP Based on Hershfield's Method

The statistical method developed by Hershfield [35,36] gives a single value of the PMP. A simple method is proposed here to take into account the uncertainty of the PMP estimator arising from the uncertainty of the sample mean and sample standard deviation.

28.5.1 Assumptions and Derivations

Referring to the original equation used by Hershfield [35], we observe that the PMP is a function of the sample mean $\overline{X}_n$, the sample standard deviation S_n, and the coefficient K. Let us denote by $\hat{P}$ the estimator of the PMP such that

$$\hat{P} = \overline{X}_n + K S_n \tag{28.1b}$$

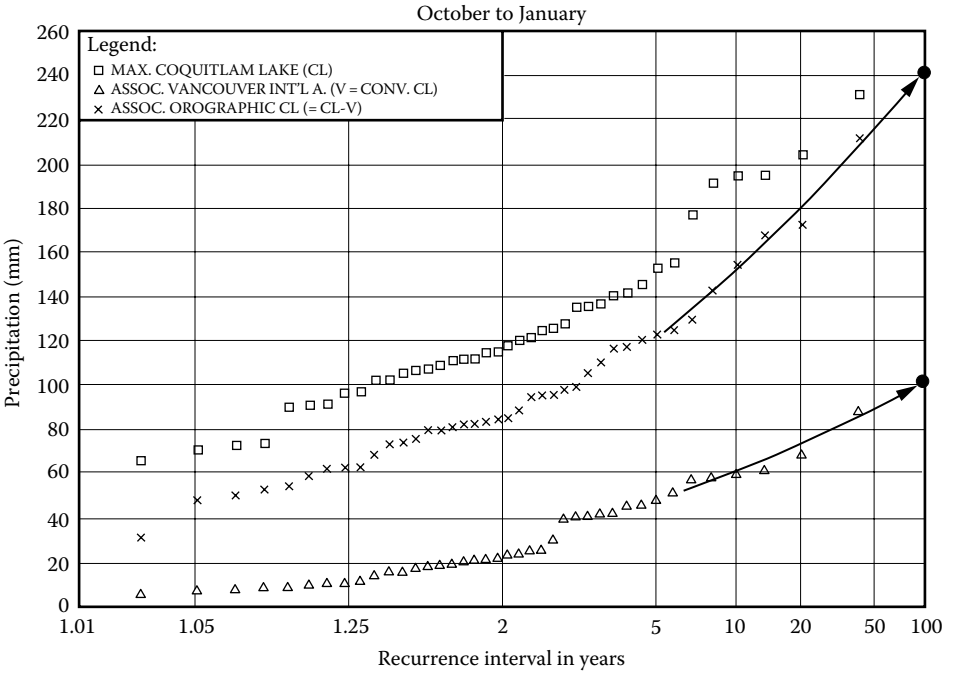

FIGURE 28.3 Empirical frequency distribution of annual maxima of daily precipitation at Coquitlam Lake (CL, square symbol) and their orographic (x symbol) and convergence (triangular symbol) components. (From Klemes, V. et al., *Dam Safety*, 1, 1992. With permission.)

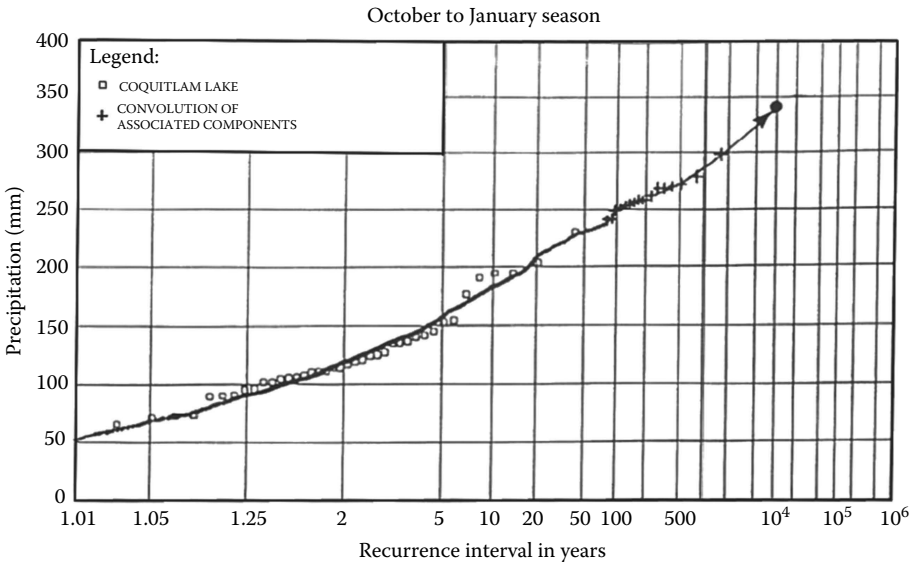

FIGURE 28.4 Empirical frequency distribution of annual maxima of daily precipitation at Coquitlam Lake obtained from the 1600 combinations of the orographic and convergence components. (From Klemes, V. et al., *Dam Safety*, 1, 1992. With permission.)

where n represents the sample size (number of years of data). Also let us recall that

$$\bar{X}_n = \frac{1}{n}\sum_{i=1}^{n} X_i \text{ and } S_n = \sqrt{\left[\frac{1}{(n-1)}\right]\sum_{1}^{n}(X_i - \bar{X}_n)^2}$$

where $X_1, X_2, \ldots, X_n$ is a random sample from an unknown distribution with population mean μ and variance σ^2. Because $\bar{X}_n$ and S_n are uncertain quantities and considering K as a constant (i.e., a maximum value corresponding to the duration of the storm, the value of $\bar{X}_n$, and the region where the basin of interest is located), one can calculate the mean and the variance of the PMP estimator $\hat{P}$. It may be worthwhile mentioning that a constant value of K is considered following Hershfield's approach in which a value of K is established after analyzing many data of historical storms that have occurred in the region under study. Thus, the uncertainty associated with K is accounted for by using an envelope function and as such K is a constant. And the remaining uncertainty is associated with $\bar{X}_n$ and S_n, which is the main subject of the argument herein.

The expected value of the estimator of the PMP, $\hat{P}$, is equal to

$$E(\hat{P}) = E(\bar{X}_n) + KE(S_n) \tag{28.2a}$$

It is clear that $E(\bar{X}_n) = E\left[(1/n)\sum_{1}^{n} X_i\right] = (1/n)\sum_{1}^{n} E(X_i) = \mu$. Likewise, it may be shown that $E(S_n) = \Gamma(n/2)\sigma/\sqrt{(n-1)/2}\,\Gamma[(n-1)/2]$ [42] where μ and σ represent the mean and the standard deviation of the population, respectively, and $\Gamma(a)$ represents the incomplete gamma function with argument a. Then (28.2a) may be written as

$$E(\hat{P}) = \mu + K\frac{\Gamma(n/2)}{\sqrt{(n-1)/2}\,\Gamma[(n-1)/2]}\sigma \tag{28.2b}$$

Note that in estimating $E(\hat{P})$ for an actual case, the population quantities μ and σ are replaced by their corresponding sample estimates (after the appropriate adjustments for outliers as needed as suggested by Hershfield).

The variance of the PMP estimator $\hat{P}$ of (28.1b) can be calculated as [52]

$$Var(\hat{P}) = Var(\bar{X}_n) + K^2 Var(S_n) + 2KCov(\bar{X}_n, S_n) \tag{28.3a}$$

Since $X_1, X_2, \ldots, X_n$ is a random sample, it is clear that $Var(\bar{X}_n) = \sigma^2/n$. Also it may be shown that the normal approximations for determining $Var(S_n)$ and $Cov(\bar{X}_n, S_n)$ are as follows: $Var(S_n) \approx \sigma^2/2(n-1)$ and $Cov(\bar{X}_n, S_n) \cong 0$ [42]. Then (28.3a) may be approximated as follows:

$$Var(\hat{P}) \cong \frac{\sigma^2}{n} + K^2\frac{\sigma^2}{2(n-1)} = \frac{\sigma^2}{n}\left[1 + \frac{nK^2}{2(n-1)}\right] \tag{28.3b}$$

And the standard deviation of the PMP estimator $\hat{P}$ is

$$\sigma(\hat{P}) \cong \frac{\sigma}{\sqrt{n}}\sqrt{1 + \frac{nK^2}{2(n-1)}} \tag{28.4}$$

The referred approximations $Var(S_n) \approx \sigma^2/2(n-1)$ and $Cov(\bar{X}_n, S_n) \cong 0$ are known to be valid where the underlying distribution of the random variable X is normal, that is, $N(\mu,\sigma^2)$ [42]. However, extreme hydrologic events, such as annual maximum precipitation, are generally skewed, and one must check

whether the referred normal approximations for determining $Var(S_n)$ and the covariance $Cov(\bar{X}_n,S_n)$ are still valid for skewed variables. Thus, a limited simulation experiment has been conducted for checking the foregoing approximations and introducing the needed corrections as appropriate. For this purpose, the GEV type 1 or Gumbel distribution was assumed as the underlying distribution of annual maximum precipitation.

Firstly, to verify the approach, 1000 samples of size $n=15$ were generated from the standard normal distribution and determined from each sample $\bar{X}_n(i)$ and $S_n(i)$, $i=1,\ldots,1000$, that is, the sample mean and standard deviations, respectively. Then, based on the pair of 1000 values, the variance $\hat{\sigma}^2(S_n)$ and covariance $\hat{Cov}(\bar{X}_n,S_n)$ were estimated. The results from the simulated samples gave $\hat{\sigma}^2(S_n)=0.035$ and $\hat{Cov}(\bar{X}_n,S_n)=0.00062$, while the theoretical normal approximations give $Var(S_n)=\sigma^2/2(n-1)=0.0357$ and $Cov(\bar{X}_n,S_n)=0$. Hence, the simulation results indicate that even for a short sample, that is, $n=15$, the approximations for obtaining $Var(S_n)$ and $Cov(\bar{X}_n,S_n)$ are correct (as expected).

For the Gumbel distribution, the CDF is given by $F(x;\underline{\theta})=\exp\left\{-\exp\left[-(x-x_0)/\alpha\right]\right\}$ in which $\underline{\theta}=\{x_0,\alpha\}$ is the parameter set where x_0 is the location parameter and $\alpha>0$ is the scale parameter [72]. Thus, Gumbel random numbers were generated by $x=x_0-\alpha\ln(-\ln u)$ in which u is a uniform (0,1) random number. The simulation experiments were made assuming that $\alpha=1$ and $x_0=1.9878$, 0.7053, 0.06405, and –0.256575, which correspond to coefficients of variation $\eta_X=0.5$, 1.0, 2.0, and 4.0, respectively (note that for $\alpha=1$, the population variance of the Gumbel distribution is $\sigma^2=1.645$.) Also in this case, 1000 samples were simulated for sample sizes $n=15$, 50, 100, and 150 and the variance $\hat{\sigma}^2(S_n)$ and correlation coefficient $\hat{\rho}(\bar{X}_n,S_n)$ determined. Table 28.2 summarizes and compares the results obtained for the variance and the correlation coefficient using the formulas that are valid for the normal distribution and using simulation, assuming the Gumbel distribution. In Table 28.2, the rows corresponding to $Var(S_n)=\sigma^2/2(n-1)$ were obtained based on the assumed values of $\sigma^2=1.645$ and n (e.g., for $n=15$, $Var(S_n)=0.05875$). On the other hand, the rows corresponding to simulation were obtained from the

TABLE 28.2 Comparison of the Variances $Var(S_n)$ and Correlation Coefficients $\rho(\bar{X}_n,S_n)$ Obtained Based on the Normal Approximations and from Generated Random Samples Gumbel Distributed with Parameters $\alpha=1$ and $x_0=1.9878$, 0.7053, 0.06405, and –0.256575 (for Coefficients of Variation $\eta_X=0.5$, 1.0, 2.0, and 4.0, respectively)

Sample Size n (1)	Variance and Correlation (2)	Approach[a] (3)	Coefficient of Variation η_X 0.5 (4)	1.0 (5)	2.0 (6)	4.0 (7)	Average (8)	Correction Factor f_n (9)
15	$Var(S_n)$	$\sigma^2/2(n-1)$	0.05875	0.05875	0.05875	0.05875	0.05875	1.752
		Simulation	0.1011	0.1026	0.1006	0.1075	0.10295	
	$\rho(\bar{X}_n,S_n)$	0.0	0.0	0.0	0.0	0.0	0.0	
		Simulation	0.5494	0.5550	0.4942	0.5388	0.5344[b]	
50	$Var(S_n)$	$\sigma^2/2(n-1)$	0.01679	0.01679	0.01679	0.01679	0.01679	1.979
		Simulation	0.0323	0.0342	0.0328	0.0336	0.03322	
	$\rho(\bar{X}_n,S_n)$	0.0	0.0	0.0	0.0	0.0	0.0	
		Simulation	0.5581	0.5097	0.5515	0.5634	0.5457[b]	
100	$Var(S_n)$	$\sigma^2/2(n-1)$	0.00831	0.00831	0.00831	0.00831	0.00831	2.133
		Simulation	0.0163	0.0173	0.0191	0.0182	0.01772	
	$\rho(\bar{X}_n,S_n)$	0.0	0.0	0.0	0.0	0.0	0.0	
		Simulation	0.5541	0.5367	0.5332	0.5516	0.5439[b]	
150	$Var(S_n)$	$\sigma^2/2(n-1)$	0.00552	0.00552	0.00552	0.00552	0.00552	2.120
		Simulation	0.0110	0.0118	0.0120	0.0120	0.0117	
	$\rho(\bar{X}_n,S_n)$	0.0	0.0	0.0	0.0	0.0	0.0	
		Simulation	0.5377	0.5628	0.5279	0.5480	0.5441[b]	

[a] $Var(S_n)=\sigma^2/2(n-1)$ and $\rho(\bar{X}_n,S_n)=0$ are based on the normal approximation.

[b] The average value of $\rho(\bar{X}_n,S_n)$ obtained from the simulated samples is about 0.542.

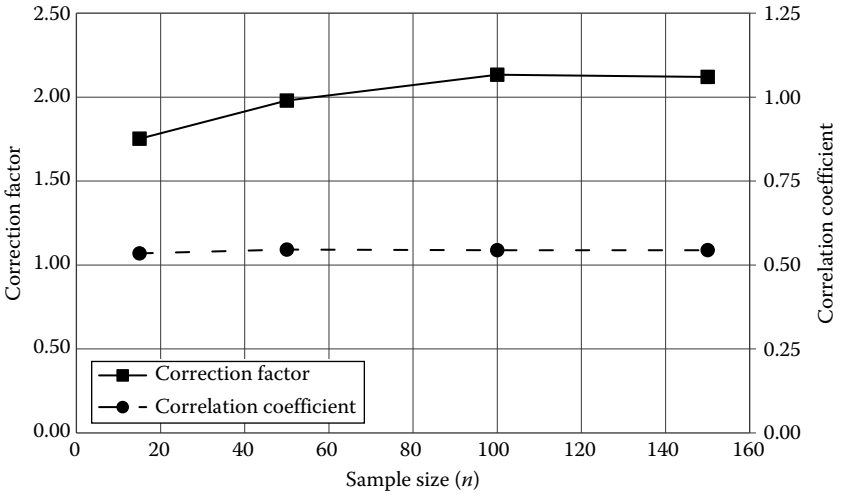

FIGURE 28.5 Variation of the correction factor f_n and the correlation coefficient $\rho(\bar{X}_n,S_n)$ as a function of the sample size n obtained by simulation using Gumbel random numbers (see Table 28.2). The correction factor f_n and the correlation coefficient $\rho(\bar{X}_n,S_n)$ are used in developing $\sigma(\hat{P})$ of (28.5).

1000 values of $S_n(i)$, $i=1,\ldots,1000$. Likewise, for $\rho(\bar{X}_n,S_n)$, the rows of zero's correspond to the result based on the normal approximation, while the values in the rows corresponding to simulation were obtained by correlating $\bar{X}_n(i)$ and $S_n(i)$, $i=1,\ldots,1000$.

First of all, one may observe that the values of $Var(S_n)$ obtained by simulation do not vary that much with the coefficient of variation η_X; thus, one may use the average figures shown in the eighth column of Table 28.2 (e.g., 0.10295 for $n=15$). The ratios of the average values (obtained by simulation) and those from the formula (based on the normal approximation) are 1.752, 1.979, 2.133, and 2.120 for $n=15$, 50, 100, and 150, respectively, as shown in the last column of Table 28.2 (e.g., for $n=15$, $f_n=0.10295/0.05875\approx 1.752$). As expected, $Var(S_n)$ varies with n, but the ratios, denoted correction factors f_n, after an initial increase for small n, seem to converge to a constant value as n increases, as shown in Figure 28.5. Thus, the factor f_n can be used to calculate $Var(S_n)$ for the Gumbel as $Var(S_n)\approx[\sigma^2/2(n-1)]\times f_n$ where f_n, for a particular value of n, can be either interpolated from the values of Table 28.2 or read of from Figure 28.5. Note that for values of $n\geq 100$, one may use $f_n\approx 2.13$, which is an average value for large n. Likewise, Table 28.2 shows that the correlation coefficient $\rho(\bar{X}_n,S_n)$, obtained from simulation, does not vary much with the coefficient of variation η_X nor with the sample size n (Figure 28.5); thus, an average figure such as 0.542 may be a reasonable correlation to use for the Gumbel distribution (Table 28.2).

Therefore, (28.4) was modified so as to consider the corrections pertaining to the variance $Var(S_n)$ and the covariance $Cov(\bar{X}_n,S_n)$ as described previously. The covariance term can be written as

$$Cov(\bar{X}_n,S_n)=\sigma(\bar{X})\sigma(S_n)\rho(\bar{X}_n,S_n)=\frac{\sigma}{\sqrt{n}}\frac{\sigma\sqrt{f_n}}{\sqrt{2(n-1)}}\rho(\bar{X}_n,S_n)$$

and using $\rho(\bar{X}_n,S_n)\approx 0.542$, one can rewrite (28.4) as

$$\sigma(\hat{P})\cong\frac{\sigma}{\sqrt{n}}\sqrt{1+\frac{nK^2f_n}{2(n-1)}+1.084\left[\frac{nK^2f_n}{2(n-1)}\right]^{1/2}} \tag{28.5}$$

which is the standard deviation of the PMP estimator $\hat{P}$ after the corrections as described previously that are applicable for skewed distributions such as the Gumbel distribution (the assumed distribution here).

28.5.2 Design PMP and Risk

Considering the uncertainty of the mean $\overline{X}_n$ and the standard deviation S_n and the ensuing uncertainties of the PMP estimator $\hat{P}$, one can estimate design values of the PMP by

$$\hat{P}_d = E(\hat{P}) \pm c\,\sigma(\hat{P}) \tag{28.6}$$

where
$\hat{P}_d$ represents a design PMP value
$c > 1$

In other words, $\hat{P}_d$ is a quantile of the uncertain quantity $\hat{P}$ of which we do not know its distribution but only the estimate of its mean $E(\hat{P})$ and the estimate of its standard deviation $\sigma(\hat{P})$. Furthermore, in order to have an approximation to the probability that the PMP estimator $\hat{P}$ may be smaller or greater than the said quantile $\hat{P}_d$, one can apply Chebyshev's inequality [52], which can be expressed as

$$P[E(\hat{P}) - c\,\sigma(\hat{P}) < \hat{P} < E(\hat{P}) + c\,\sigma(\hat{P})] \geq 1 - \frac{1}{c^2} \tag{28.7}$$

This inequality gives a bound of the probability that does not depend on the distribution of $\hat{P}$. As expected, the probability bound is conservative since one only knows the mean and the standard deviation of $\hat{P}$ but not its distribution. The applicability of (28.7) is illustrated in the case study presented in the following section.

The proposed method for determining the PMP estimate, the corresponding uncertainty, the design PMP, and associated probability bounds may be summarized as follows: (a) adjust $\overline{X}_n$ and S_n for effect of outlier as in the original method by Hershfield; (b) select K as a function of $\overline{X}_n$, the storm duration, and the study region; (c) estimate the expected value of the PMP estimator $E(\hat{P})$ by using (28.2b) and multiply this value by an adjustment as in step (e) of Hershfield's method as described previously at the end of Section 28.3.2; (d) estimate the standard deviation of the PMP estimator $\sigma(\hat{P})$ by using (28.5) where the correction factor f_n is obtained by interpolating from Table 28.2 or from Figure 28.5; (e) use (28.6) to obtain design values $\hat{P}_d$ of the PMP; and (f) use Chebyshev's inequality (28.7) for obtaining probability bounds of the PMP estimator $\hat{P}$. This modified method is further illustrated in the following case study.

28.5.3 Case Study

The case study refers to the design of the spillway capacity of a high dam that is being constructed at the Tona River north of Bucaramanga, Colombia, near its confluence with the Surata River (the area of the basin at the dam site is 195 km^2 and the mean slope of Tona River is about 7%.) For this purpose, the Metropolitan Aqueduct for Bucaramanga contracted the pertinent hydrologic studies with leading consulting firms in Colombia. The consultants and designers of the dam decided using the PMP and PMF approach for estimating the design flood for the spillway. The hydrologic data and basic studies performed by the consultants considered estimating the PMP for various storm durations, and the methods utilized included storm maximization and transposition and Hershfield's original statistical method. However, in this case study, only the statistical method due to Hershfield's including the proposed modifications to account for the uncertainty (as described previously) is compared and discussed. The statistical estimates were based on 15 years of annual maximum daily precipitation recorded at the Martín Gill station (located within Tona's River basin) where $\overline{X}_n = 66.5$ mm, $S_n = 24.5$ mm, and $n = 15$ (Table 28.3).

The main results of applying the original (statistical) method by Hershfield and those obtained using the proposed method of PMP with uncertainty are included in Table 28.3. The first line of results in Table 28.3 corresponds to the estimates based on the original method of Hershfield as described previously. The adjustments for the mean and the standard deviation to account for the limited sample size

TABLE 28.3 Comparison of the 24 h PMP for Tona River Obtained Based on Hershfield's Original Method and Based on the Proposed Method Considering Uncertainty Assuming the Normal and Gumbel Approximations for Calculating $Var(S_n)$ and $Cov(\overline{X}_n, S_n)$

Mean $\overline{X}_n$ (mm)		Std. Deviation S_n (mm)			Traditional Hershfield's PMP (mm) from (28.1a)	PMP with Uncertainty (mm)		
Original	Adjusted Hershfield	Original	Adjusted Hershfield	K		$E(\hat{P})$ (28.2b)	$\sigma(\hat{P})$ (28.4)	$\hat{P}_d^*$ (28.6)
66.5	68.5	24.5	27.7	8.9	369[a]			
66.5		24.5		8.9		328[b]	41.7	370[c]
								411[d]
								453[e]
								495[f]
							From (28.5)	
							58.2	386[c]
								444[d]
								503[e]
								561[f]

[a] PMP = $(68.5 + 8.9 \times 27.7) \times 1.17 \approx 315 \times 1.17 \approx 369$ mm (using an adjustment factor 1.17).
[b] The $E(\hat{P})$ obtained from (28.2b) is multiplied by the adjustment factor 1.17.
$\hat{P}_d$ of (28.6) considering the upper limit, that is, $\hat{P}_d^* = E(\hat{P}) + c \times \sigma(\hat{P})$ in which
[c] $c = 1$.
[d] $c = 2$.
[e] $c = 3$.
[f] $c = 4$.

(as suggested by Hershfield) were made using the graphs available at WMO [83], (Figure 4.4) that gave adjustment factors equal to 1.03 and 1.13, for the mean and the standard deviation, respectively. Thus, the adjusted values of the sample mean and standard deviation are 68.5 and 27.7 mm, respectively (Table 28.3). In addition, the value of the frequency factor $K = 8.9$ was obtained from the results for Colombia for 24 h duration of precipitation [50]. Then using the foregoing values, one can obtain from Equation 28.1a the value of PMP = 315 mm. Note that Hershfield [35] recommended an additional adjustment of 1.13 on the estimated PMP value to account for the difference between the daily maximums and the 24 h maximums. But other recent studies such as those in Spain [8] and Great Britain [20] gave adjustment factors of 1.16 and 1.17, respectively. Hence, in all subsequent calculations, the factor 1.17 was applied. Therefore, the PMP adjusted value using Hershfield's method becomes 369 mm as shown in Table 28.3 (see the notes at the bottom of table). One must also note that no adjustments for outliers were made because the analysis of the 15 years of data did not show any evidence of outlying observations. In addition, Hershfield's method for adjusting for outliers gave adjustment coefficients for the mean and the standard deviation that were practically equal to one in both cases.

While Hershfield's adjustments for the mean and the standard deviation have been a way of taking into account the limited sample size of the available precipitation records, however. Hershfield's method does not give any information on the uncertainty of the PMP estimates, that is, the standard error of the estimator $\hat{P}$ of (28.1b), which arises from the uncertainties of the estimators $\overline{X}_n$ and S_n. As suggested in Section 28.5.1 previously, those estimates with uncertainties can be obtained approximately by (28.2b), (28.4), and (28.5), depending on the approximations utilized. For example, the second row of results in Table 28.3 shows that $E(\hat{P}) = 328$ mm, which is obtained from (28.2b) based on $\overline{X}_n = 66.5$, $S_n = 24.5$, $n = 15$, and $K = 8.9$ and then multiplying the result from (28.2b) by the adjustment factor 1.17 as described previously. Next (column before the last one) are the results obtained for $\sigma(\hat{P})$ applying (28.4), based on the normal approximation that gave $\sigma(\hat{P}) = 41.7$ mm and (28.5) based on the Gumbel approximation, which gave $\sigma(\hat{P}) = 58.2$ mm. In addition, the last column in Table 28.3 shows results of the design PMP $\hat{P}_d$ of (28.6) considering four values of c, that is, $c = 1$, $c = 2$, $c = 3$, and $c = 4$. First, the concepts based on the results obtained using the normal approximations (for $Var(S_n)$ and $Cov(\overline{X}_n, S_n)$) are illustrated, and subsequently the results

obtained based on the Gumbel approximation are discussed. One may observe that (28.6) with $c = 1$ and the + sign, that is, $\hat{P}_d^* = E(\hat{P}) + \sigma(\hat{P})$, gives $\hat{P}_d^* = 370$ mm, which is the least conservative estimate and is about the same value obtained using Hershfield's original method, that is, PMP = 369 mm. Obviously, the most conservative estimate included in Table 28.3 corresponds to $c = 4$, that is, $\hat{P}_d^* = 495$ mm. The decision for selecting a design value of the PMP based on statistical concepts must consider the fact that the estimates are based on statistics that are computed from a limited sample, and in this case study, the sample is only 15 years long. Thus, the selected design value must be such that the probability of that value being exceeded must be small.

The Inequality 28.7 provides some useful information that may help in selecting the design PMP value. Thus, applying (28.7) and $\sigma(\hat{P})$ based on (28.4) gives the following:

$$\text{For } c = 1, \quad P[286 < \hat{P} < 370] \geq 0.0$$

$$\text{For } c = 2, \quad P[245 < \hat{P} < 411] \geq 0.75$$

$$\text{For } c = 3, \quad P[203 < \hat{P} < 453] \geq 0.89$$

$$\text{For } c = 4, \quad P[161 < \hat{P} < 495] \geq 0.94$$

These results must be interpreted as follows. For example, for $c = 3$, the probability that the PMP estimator $\hat{P}$ is bigger than 453 mm and smaller than 203 mm is less than 11%. For comparison, if the true underlying distribution of $\hat{P}$ were normal, then that probability would be less than 0.3% (instead of 11%). Likewise, if we take instead $c = 4$, then in this case the foregoing probabilities would be less than 6% and 0.01%, respectively. Naturally, one could select even higher values of c and obtain more conservative values of the PMP with smaller risks of exceedances.

The foregoing analysis of the results included in Table 28.3 suggests that the PMP estimates considering the effect of uncertainty and the normal approximations vary in the range of 370–495 mm (the top four values shown in the last column of Table 28.3). The lowest value 370 mm corresponds to the case where the PMP is obtained simply by adding one standard deviation to the estimated mean value $E(\hat{P})$. Without further information beyond the mean $E(\hat{P})$ and the standard deviation $\sigma(\hat{P})$, the probability bound previously suggests that it is very likely (in fact almost certain) that such value of 370 mm will be exceeded because of the uncertainty associated with estimating $\overline{X}_n$ and S_n that are based on only 15 years of records. On the other hand, the value of 495 mm corresponds to a conservative estimate, that is, it is less likely that it will be exceeded because of the uncertainties associated with $\overline{X}_n$ and S_n. Thus, the results show a major difference between the single value of the PMP (equal to 369 mm) that one obtains applying the original method of Hershfield and the range of PMP values obtained by the proposed method that takes into account the effect of uncertainty and their associated probabilities of exceedances.

The calculations and analysis of design PMP and probability bounds of the previous discussion have been made using (28.4) for calculating the standard deviation of the PMP estimator $\sigma(\hat{P})$, which assumes the normal approximations for the variance $Var(S_n)$ and the covariance $Cov(\overline{X}_n, S_n)$ as described previously. However, using $\sigma(\hat{P})$ of (28.5) will give more accurate results if the distribution of the annual maximum daily precipitation is skewed as one may expect. Thus, for comparison, we applied (28.5) where $n = 15$, $\sigma = 24.5$, $K = 8.9$ (Table 28.3), and $f_{15} = 1.752$ (see Section 28.5.1 and Table 28.2), which gives $\sigma(\hat{P}) = 58.2$ mm, an amount that is about 40% higher than that based on (28.4). However, the overall increase in the design value of the PMP of (28.6) is not as high. Thus, we computed four design values of the PMP based on (28.6) for $c = 1$, 2, 3, and 4, and the values obtained are those shown in the lower portion of the last column of Table 28.3. For illustration, for $c = 1$, we get $\hat{P}_d^* = 386$ mm, which compared to the value 370 mm (Table 28.3) represents an increase of about 4%. Likewise, the percent increases for the other cases shown in Table 28.3 are about 8%, 11%, and 13% for $c = 2$, 3, and 4, respectively.

One must note that the previous analysis clearly indicates the striking difference between the PMP value obtained using the traditional Hershfield's method (PMP = 369 mm) and the PMP values that are obtained using the proposed method that accounts for the uncertainties involved, which gives values varying in the range of 386–561 mm (lower portion of the last column in Table 28.3). These values (386, 444, 503, and 561 mm) are, respectively, about 5%, 20%, 36%, and 52% higher than the single value of PMP obtained with the original Hershfield's method. Furthermore, the proposed method, which includes the probability bounds, suggests that using say the smaller value of 386 mm as the design PMP (which is even 5% bigger than the 369 mm PMP obtained from the original Hershfield's method) would not be wise because it is certain that it will be exceeded. Therefore, a bigger value must be selected considering the associated exceedance probabilities (risk) as described previously.

28.6 PMF Estimation and Uncertainty

28.6.1 PMF Estimation from PMP

Several books and manuals have documented the procedures for determining the PMF from the PMP [14,57,65]. The following list is a simplified summary of the procedures followed by USBR and many other agencies in the United States [73]: (1) divide the basin into subbasins as needed and determine the drainage areas; (2) estimate the PMP; (3) arrange the PMP into a storm rainfall pattern; (4) estimate the rainfall losses due to surface detention and infiltration, and determine the rainfall excess for each time interval; (5) route the rainfall excess through each subbasin to estimate the flood hydrograph for each subbasin; (6) add to the flood hydrograph of each subbasin the corresponding base flow, flow from prior storms, as the case may be, to get an estimate of the flood hydrograph for each subbasin; (7) route the flood hydrograph from each subbasin to estimate the PMF at the point of interest (e.g., site of a dam); and (8) route the PMF through the reservoir storage, outlets, and spillway to obtain estimates of maximum storage, elevation, discharges, and durations at the project site. The procedures also include comparisons of applicable envelope curves of flood peaks and volumes if available.

Some of the previous steps (e.g., steps 4 through 7) may be computed using a given rainfall–runoff model. For this purpose, a number of models have been developed for the past several decades. For example, in the United States, the Hydrologic Engineering Center (HEC)-1 [75] and HEC-Hydrologic Modeling System (HEC-HMS) [76] models are widely utilized in practice for flood hydrograph computations. These models are based on the unit hydrograph concept, and also the flood hydrograph and runoff (FHAR) model promoted by the USBR uses the unit hydrograph [73]. The unit hydrograph approach represents the rainfall–runoff process as a linear system. Also, various rainfall–runoff models that consider the underlying nonlinear mechanism of the rainfall–runoff processes have been proposed in literature such as CASC2D [40] and Two-dimensional runoff, erosion, and expert model (TREX) [80].

In addition, the advances in GIS-based computer models in the past decades brought further capabilities for analyzing runoff hydrographs as a function of the watershed characteristics and enhancing the applicability of distributed modeling in watershed hydrology. For example, CASC2D [39,40,41] is a raster-based watershed model that accounts for the spatial variability in the watershed topography, soil type, and land use. The CASC2D model has been extended to TREX by Velleux et al. [80] to simulate the transport and fate of metals in relation to rainfall–runoff and sediment transport at the watershed scale. England et al. [23] applied TREX to simulate extreme storms including the PMP on the Upper Arkansas watershed covering 12,000 km^2 in Colorado.

As one may observe from the previous summarized steps, estimating the PMF for a specific basin (project) involves a wide range of factors such as rainfall depth and duration (PMP), temporal pattern of the PMP, spatial distribution of the PMP, centering of the storm over the basin, lag time and unit hydrograph estimation, loss rates estimation, antecedent flooding before the onset of the PMP (previous storms and snowmelt as the case may be), and flood routing through the basin channels and reaches. Each of the referred factors of the previous discussion and the calculation steps to estimate the PMF involve some

degree of uncertainty. While this issue has been recognized in literature, still the knowledge for quantifying the various uncertainties and their effects on the PMF is lacking. Bondelid et al. [6] indicated that the uncertainty in estimating the lag time may cause errors in estimating the maximum floods of the order of 75%. Useful references on uncertainties of time of concentration and lag time for various types of watersheds and formulas commonly utilized in practice are available [29,48,49,74]. In the following sections, we illustrate the variability of the PMF based on sensitivity analysis and Monte Carlo simulation.

28.6.2 Sensitivity Analysis

The TREX model is applied for sensitivity analysis of some of the model parameters on the PMF. For this purpose, the Semenyih watershed (236 km^2), which is located in the state of Selangor in Malaysia, is utilized. The watershed is partially used for agriculture but urbanization (residential and industrial) development has rapidly transformed the area in recent decades. The topography of the watershed has been discretized with 29,139 cells at a 90 m × 90 m grid scale. The digital elevation model (DEM) data for the study site (Figure 28.6a) were obtained from the Department of Surveying and Mapping of Malaysia. The lowest elevation at the outlet is 40 m above sea level, while the highest point reaches 1100 m at the upstream end of the watershed. The average terrain slope is about 45% and ranges between 4% and 85% with very steep mountains overhanging flat and wide valleys (Figure 28.6a). The DEM also allowed the delineation of the channel network of the watershed where the total stream length reached about 36 km. Four soil types (Figure 28.6b) and six land uses (Figure 28.6c) were included in the raster-based GIS representation of the watershed. The soil types allowed the definition of the effective hydraulic conductivity K_h, and the land use types enabled the definition of the land surface Manning's roughness coefficients n.

The April 13, 2003, storm was used for model calibration where the precipitation and flow records were obtained from the Department of Irrigation and Drainage of Malaysia. The calibration procedure focused on properly simulating peak flow, discharge volume, and time to peak at the outlet. The TREX model has several parameters such as hydraulic conductivity, Manning's roughness coefficient, interception depth, capillary suction head, and soil moisture deficit. These parameters were adjusted during calibration so as to achieve good agreement between the measured and simulated flow. The antecedent moisture condition of the watershed was assumed dry. Table 28.4 gives the values of the calibrated parameters K_h and n for the specified type of soils and land use (the other parameters are omitted).

Several studies have been made to estimate the PMP for Malaysia. For example, Poon and Hwee [64] reviewed earlier studies and Figure 28.7 shows the PMP estimates for various storm durations in the state of Selangor (S-PMP). For comparison, the figure also shows the rainfall depths for the 100-year-return period [18] and the world's greatest precipitation events [38]. For the purpose of this study, the 16 h precipitation depths were utilized as input to the calibrated TREX model. These rainfall events are summarized in Table 28.5. TREX calculates the distribution of flow depth on each calculation cell as a function of time. To illustrate the results, Figure 28.8 shows the calculated distribution of the peak flow depth on the Semenyih watershed at the time of the peak discharge during the S-PMP. The PMF hydrograph at the outlet of the basin is shown in Figure 28.9. For comparison, this figure also shows the flood hydrographs calculated for the 100-year and the world's greatest storm events (Table 28.5). Also for comparison, the figure shows the hydrographs obtained using the HEC-HMS model (dashed lines).

Experience using the TREX model in simulating a wide range of rainfall–runoff events has shown that the most sensitive parameters are the saturated hydraulic conductivity K_h and the overland flow resistance Manning's coefficient n [22,79]. Thus, the sensitivity analysis of the PMF considered here uses the range of values of the parameters K_h and n shown as lower and upper values in Table 28.4. The combination of the upper, lower, and calibrated values of K_h and n gave a range of calculated PMF values that are summarized in Table 28.6. It shows that the PMF values vary in the range of 1245–1866 cm and the mean and standard deviation are about 1527 and 270 cm, respectively. The maximum discharge is obtained for the lowest values of K_h and n. Besides showing the variability of the computed PMF, the results also suggest that the Manning's roughness coefficient is the most important parameter controlling the flow at the outlet of the basin.

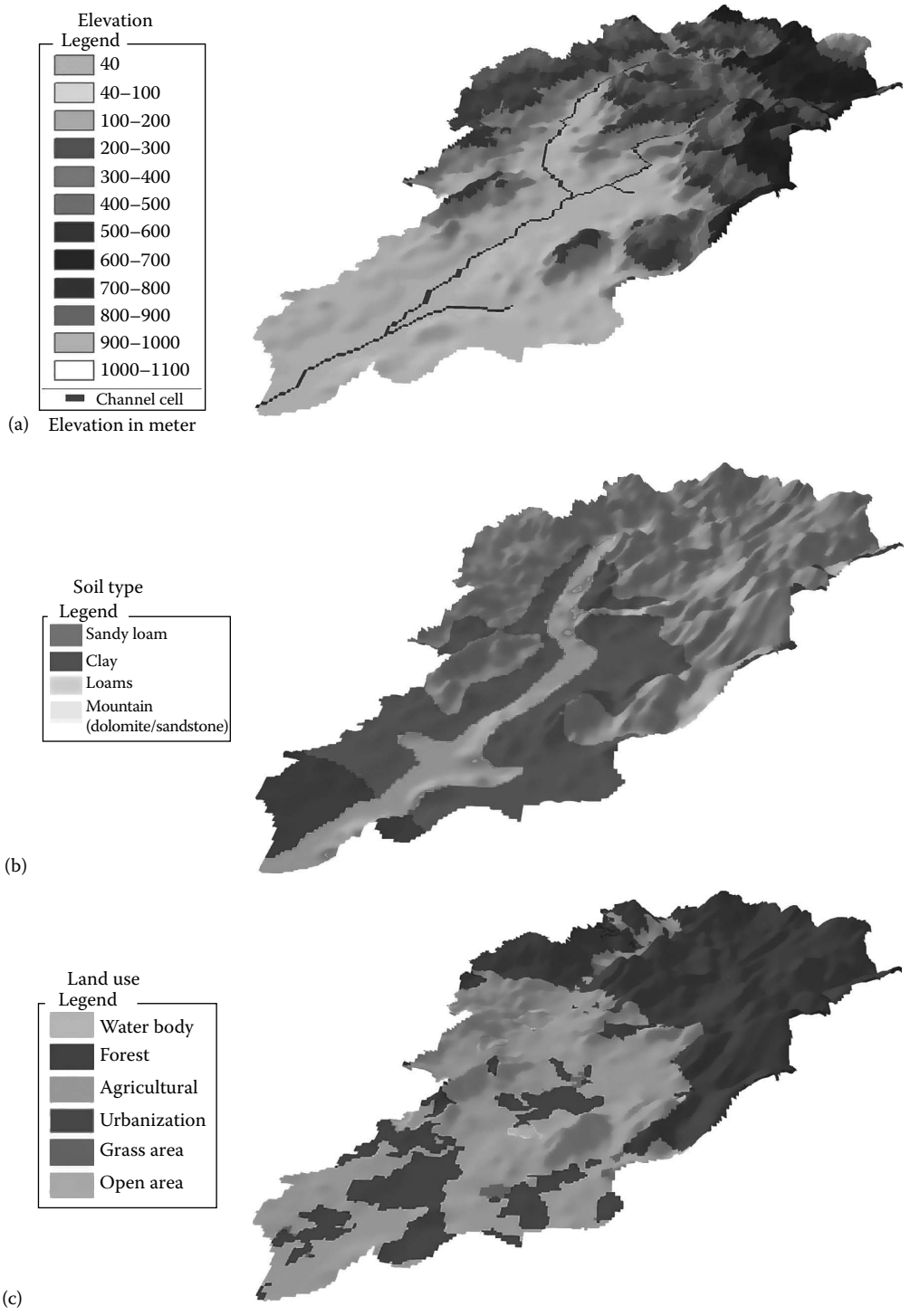

FIGURE 28.6 (a) Elevation, (b) soil type, and (c) land use for the Semenyih watershed in Malaysia.

TABLE 28.4 Hydraulic Conductivity K_h and Manning's n Values Obtained after Calibrating TREX Model for the Semenyih Watershed

Parameter	Lower	Calibrated	Upper	Soil Type/Land Use
Hydraulic conductivity K_h (m/s)	5.60×10^{-9}	1.12×10^{-8}	1.68×10^{-8}	Sandy loams
	6.35×10^{-9}	1.27×10^{-8}	1.91×10^{-8}	Loams
	1.53×10^{-9}	3.06×10^{-9}	4.59×10^{-9}	Clay
	5.90×10^{-11}	1.18×10^{-10}	1.77×10^{-10}	Mountain–limestone
Manning's n	0.050	0.100	0.150	Agriculture
	0.025	0.050	0.075	Urban/commercial
	0.100	0.200	0.300	Forest
	0.050	0.100	0.200	Grass area
	0.050	0.100	0.150	Open area
	0.020	0.040	0.060	Channel bed

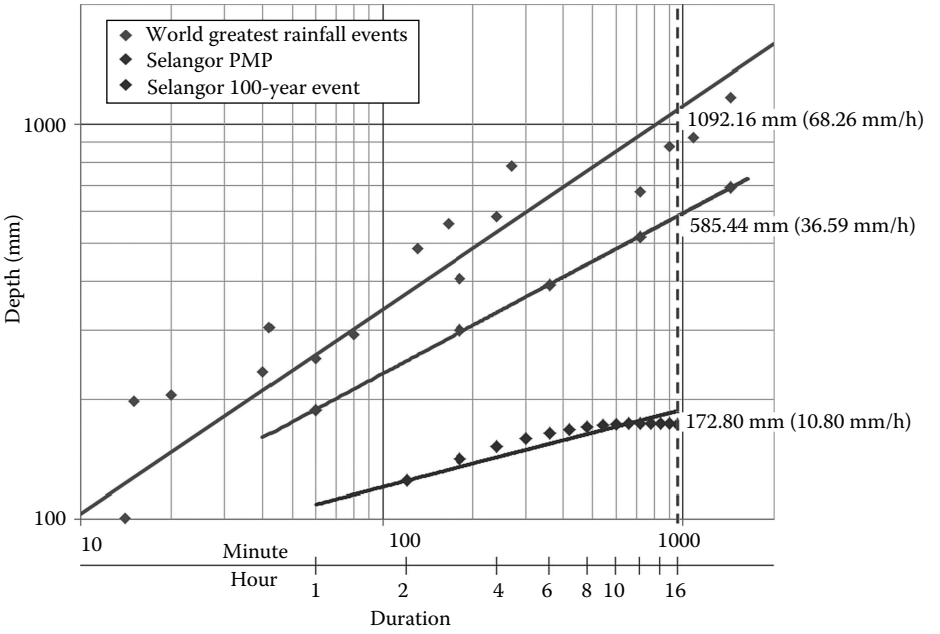

FIGURE 28.7 PMP estimates for the state of Selangor, Malaysia, for various storm durations. For comparison, the 100-year rainfall depths and the world's greatest rainfall depths are also shown.

TABLE 28.5 Precipitation Depth and Intensity and Corresponding Flood Properties Obtained from Model TREX for the 100-year, PMP, and World's Greatest Storms for the Semenyih Basin

	Precipitation		Flood Hydrograph Results	
Events	Depth (mm)	Intensity (mm/h)	Peak Discharge (cm)	Time to Peak (24 h)
100-year	173	11	223	23:36
PMP	585	37	1484	19:06
World's greatest rainfall	1092	68	3686	17:30

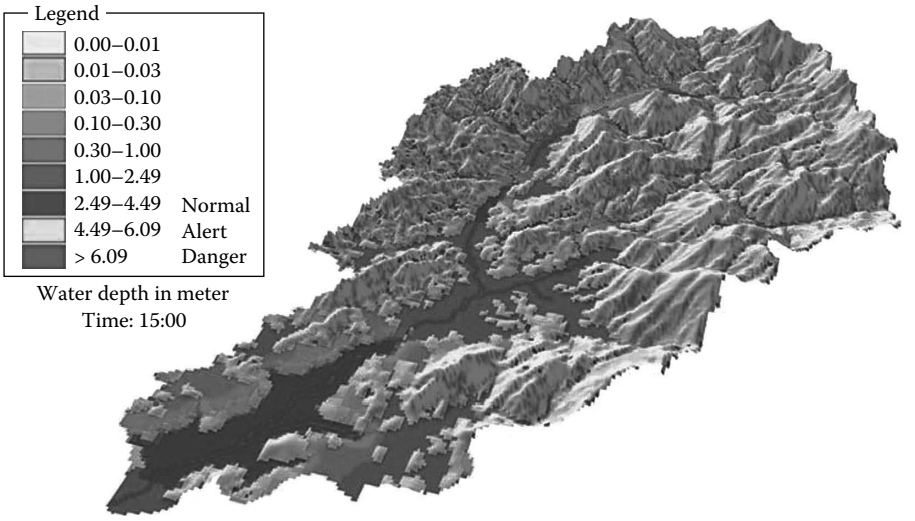

FIGURE 28.8 Spatial distribution of peak flow depth in meters for the PMP event (37 mm/h at 16 h duration).

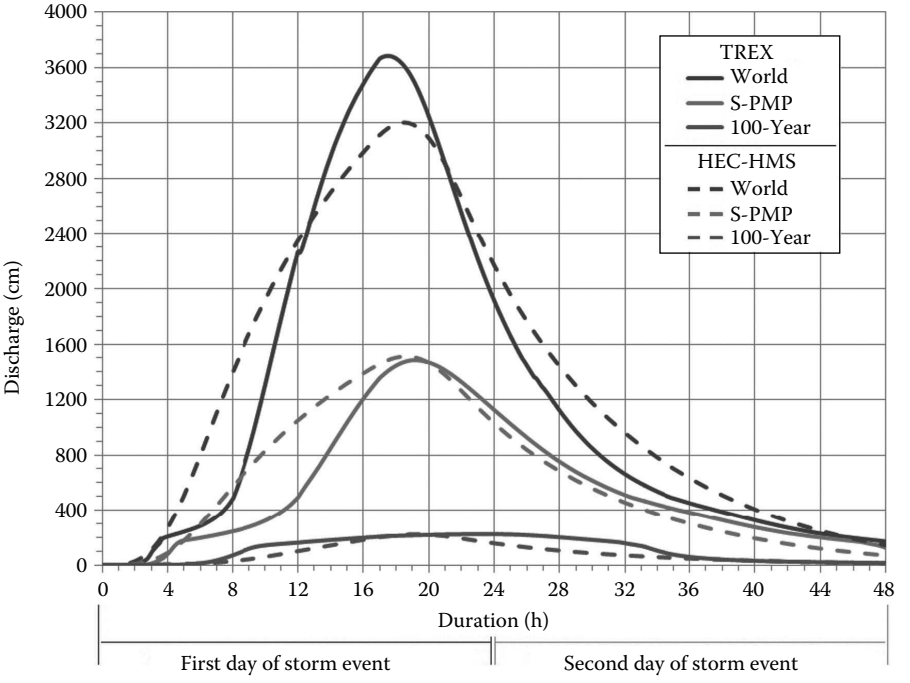

FIGURE 28.9 Flood hydrographs obtained from TREX and HEC-HMS models using the 16 h 100-year, PMP, and world's greatest storms.

28.6.3 Monte Carlo Analysis

A Monte Carlo method has been developed to determine the uncertainty of the PMP in a joint effort by the USBR and Washington state [3]. Since then, a number of articles and applications have been made [70]. In Barker et al. [3], the various factors involved in estimating the PMF including some of

TABLE 28.6 Sensitivity Analysis of the PMF Obtained from the TREX Model for Various Combinations of the Parameters for the Semenyih Watershed

Hydrologic Model Parameters		Flood Peak (cm)
Hydraulic Conductivity K_h	Manning's n	
Calibrated values		1474
Lower limit	Lower limit	1866
Upper limit	Upper limit	1242
Lower limit	Upper limit	1249
Upper limit	Lower limit	1859
Calibrated value	Lower limit	1859
Calibrated value	Upper limit	1245
Upper limit	Calibrated value	1476
Lower limit	Calibrated value	1472
Mean		1527
Standard deviation		270

the hydrologic model input parameters were treated as variables with specified distributions. Values of the various factors and parameters were drawn at random from the corresponding distributions that were then utilized for estimating the PMF. The overall method is summarized in the following steps: (a) select the season of occurrence of the PMP; (b) select all hydrometeorological, hydrologic, and hydraulic parameters that are dependent upon season of occurrence; (c) select all parameters that are independent of other parameters; (d) select all hydrologic and hydraulic parameters that are dependent upon other flood model parameters; (e) estimate the flood; (f) repeat steps (a) through (e) a large number of times, for example, 500 times; and (g) do statistical analysis of the estimated flood values.

The method summarized previously has been applied to the Bumping Lake basin located in the Cascade Mountains in Washington state [3]. The basin area is 67 miles^2, the topography ranges from 3400 ft at the dam site to over 6000 ft at the headwaters near the crest of the mountains, and the mean annual precipitation varies from about 48 in. near the dam to over 70 in. at the headwaters. The PMPs were determined based on the HMR-57 [60] as 10.6 in. for 6 h, 20.6 in. for 24 h, and 32.2 in. for the 72 h. The HEC-1 program was utilized for the flood computations [75], and probability distributions were used for the following input parameters: season of occurrence of the PMP, antecedent precipitation, initial streamflow, antecedent snowpack, antecedent soil moisture, occurrence of frozen ground, minimum infiltration rate, and unit hydrograph time lag. Since the HEC-1 model utilized does not account for subsurface catchment response, appropriate additional steps were added to account for that component. Based on detailed analysis of the hydrometeorological historical data for the study region, appropriate PDFs were selected for the various input parameters as summarized in Table 28.7. The results of 500 Monte Carlo simulations based on the PMPs specified in HMR-57 (as noted previously) are shown in the frequency distribution of the PMFs in Figure 28.10. The simulated PMFs gave the following: mean PMF = 64,000 cfs and standard deviation of PMF = 7,220 cfs and a range of 45,000–84,000 cfs. Note that the PMF computed using the standard USBR approach gave a PMF equal to 71,000 cfs that is about one standard deviation above the mean of the simulated results. The results obtained suggest the uncertainty of the PMF (for the specified PMP) that arises from the uncertainty of the various hydrometeorological factors involved in estimating the PMF.

Two additional Monte Carlo studies were made where the magnitude and temporal characteristics of the precipitation input were assumed to vary in addition to the other parameters described previously [3]. In the first case, the 24 h PMP (20.6 in.) specified by HMR-57 was held constant, and the temporal characteristics were varied by examining the depth-duration curves contained in HMR-57 and the extreme storms observed in the past. The results of 500 simulations gave mean PMF = 42,300

TABLE 28.7 Probability Distributions Utilized in the Monte Carlo Method

Parameter	Probability Model
PMP season of occurrence	Beta distribution
Antecedent precipitation (bimonthly)	Beta distribution
Antecedent temperature (bimonthly)	Normal distribution
Antecedent snowpack (bimonthly)	Regression with antecedent precipitation and temperature plus error term
September 1 soil moisture deficit	Beta distribution
Minimum infiltration rate	Symmetrical beta distribution
Deep percolation rate	Symmetrical beta distribution
Unit hydrograph lag (natural variability)	Normal distribution
Unit hydrograph lag (runoff mechanism)	Linear scaling factor
Initial streamflow	Regression with antecedent precipitation plus error term

Source: Barker, B. et al., A Monte Carlo approach to determine the variability of PMF estimates, Final Report on Bumping Lake Dam for USBR Dam Safety Office, 1997. With permission.

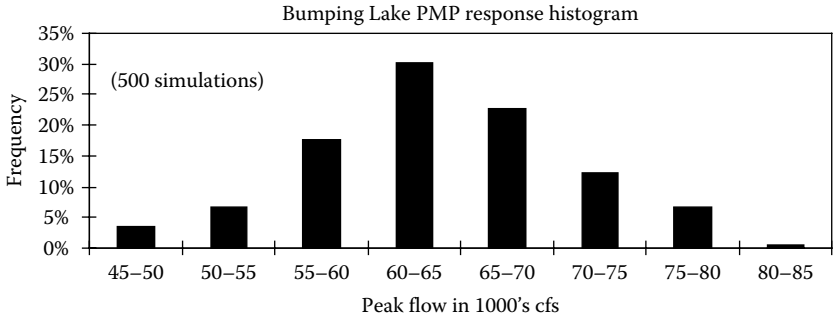

FIGURE 28.10 Relative frequency distribution of the PMFs obtained from the 500 simulations for Bumping Lake using the PMP specified in HMR-57. (From Barker, B. et al., A Monte Carlo approach to determine the variability of PMF estimates, Final Report on Bumping Lake Dam for USBR Dam Safety Office, 1997. With permission.)

cfs and standard deviation of PMF = 10,200 cfs and a range of 14,700–75,100 cfs. Figure 28.11 shows the frequency plot of the PMFs obtained. The results show the sensitivity of the peak flow to the temporal pattern of the storm, the peak precipitation intensity, and the total volume of the storm [3]. In the second case, the 24 h precipitation depth was allowed to vary for each simulation run. For this purpose, the 4-parameter kappa distribution was fitted to the historical 24 h annual maximum precipitation events. Monte Carlo simulations of the 24 h precipitation gave an AEP = $10^{-7.3}$ of the PMP, and the corresponding simulations of the flood peaks gave a frequency distribution as shown in Figure 28.12. The figure shows that the PMF (71,000 cfs) has an AEP of 1.5×10^{-8}, and the mean of the flood conditioned on the occurrence of the 24 h PMP (42,300 cfs, Figure 28.11) has an AEP of 1.8×10^{-6}. This implies that the methods that are used to develop the PMF (standard USBR procedures) give a flood that is about two orders of magnitude more rare than the 24 h PMP that was used to generate the flood [3]. The results of the simulations serve not only for quantifying the uncertainty of the PMF but also for estimating the order of magnitude of the AEP of the PMF that is estimated using the traditional approaches.

28.6.4 Statistical Alternatives for Estimating Extreme Floods (Including PMF)

In the last decades, a tendency worldwide has been towards risk-based approaches for designing flood-related structures such as flood walls and spillways [24]. As for extreme precipitation, studies of high

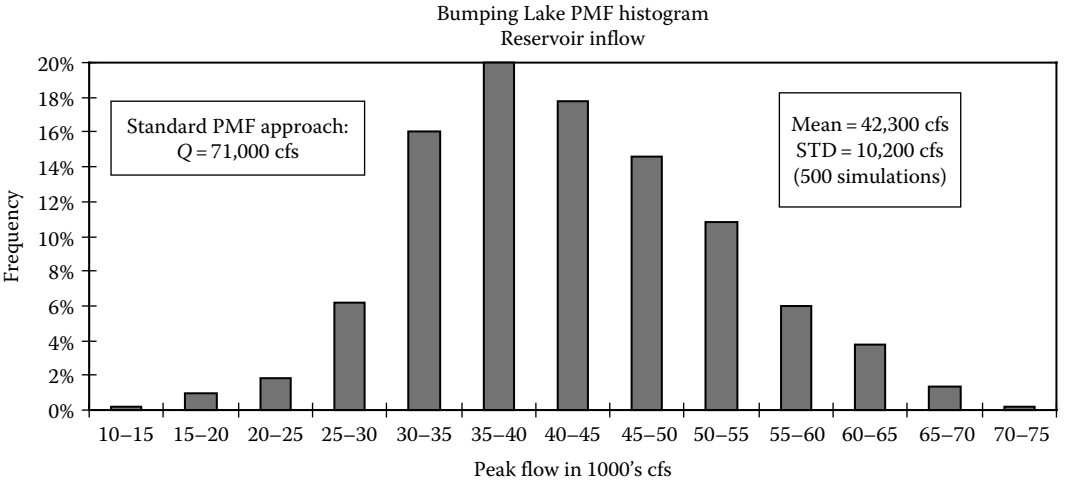

FIGURE 28.11 Relative frequency distribution of the PMFs obtained from the 500 simulations for Bumping Lake where the 24 h precipitation was held constant at the PMP, while the other variables, including the precipitation temporal pattern, varied. (From Barker, B. et al., A Monte Carlo approach to determine the variability of PMF estimates, Final Report on Bumping Lake Dam for USBR Dam Safety Office, 1997. With permission.)

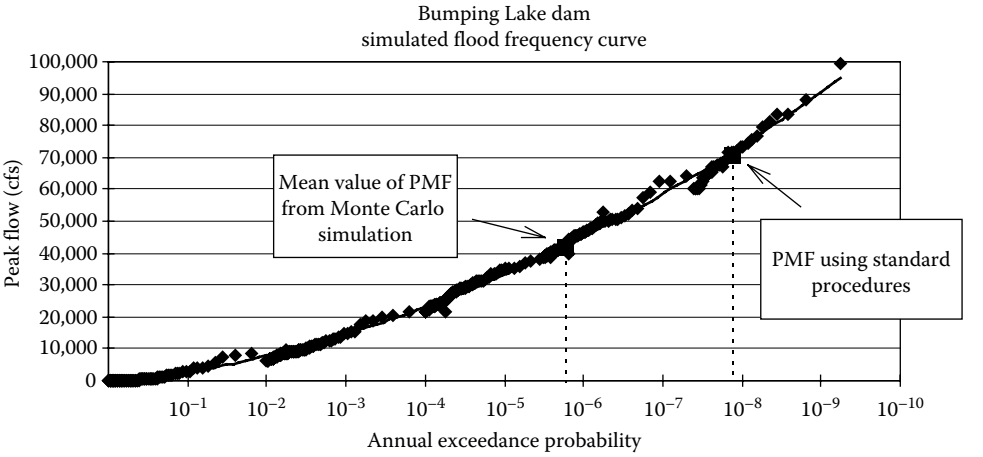

FIGURE 28.12 Frequency distribution of the flood peaks obtained by Monte Carlo simulation considering the uncertainty of the 24 h annual maximum precipitation in addition to the uncertainty of the other driving variables to estimate the flood. (From Barker, B. et al., A Monte Carlo approach to determine the variability of PMF estimates, Final Report on Bumping Lake Dam for USBR Dam Safety Office, 1997. With permission.)

return period floods based on statistical approaches have been proposed. They generally involve extrapolations of the FCs obtained from the systematic flood records including historical and paleoflood data [7,21,28,71]. However, federal and state agencies in the United States and similar organizations in other countries still use the PMF as the standard for assessing flood-related infrastructure. For example, the USBR's current policy is to use the PMF as an upper limit to hydrologic hazard curve extrapolations [78] without directly assigning an AEP to the PMF [24], that is, there is no fixed assumption for AEP of the PMF. Examples of an array of techniques developed by USBR in the last two decades can be found in Swain et al. [73]. They involve using historical and paleoflood data, mixed-population approach, expected moments algorithm (EMA), and Bayesian maximum likelihood [11,21,61].

Likewise, the USACE has been developing methods for extrapolating the flood frequency curves (FFCs) all the way to the AEP of the PMF. For example, the HEC has been developing methods for FFC extension to the level of the PMF and provides simple methods to estimate the AEP of the PMF [34]. For this purpose, the return period for the PMF is assumed to be in the range 10^{-3} to 10^{-6} and provide a simple equation to calculate the AEP of the PMF. In some cases, the extrapolation of FFCs beyond the range of the 100-year flood has been based on assuming (assigning) an AEP to the PMF. For example, the guidelines on extreme flood analysis for the Department of Transportation of Alberta, Canada, specify that the AEP for the PMF be set to 10^{-5} (100,000 years of return period) so that flood estimates for return periods of 1,000 and 10,000 years can be made [2].

28.7 Summary and Conclusions

The topic of uncertainty in estimating the PMP and PMF has been the main trust of this chapter. There are many studies documenting the various developments for estimating the PMP and PMF based on physically based (hydrometeorological) and statistical approaches. And many federal and state organizations worldwide use the PMP and PMF as standards for designing some flood-related hydraulic structures. However, in recent decades, there has been a growing concern (expressed in literature) regarding the uncertainties involved in estimating such extreme events, and the tendency has been to estimate their exceedance probabilities. In this chapter, we included some developments directed to quantify the uncertainty of the PMP and PMF. While hydrometeorological methods likely provide the best estimates of PMP, however, in many regions of the world, hydrometeorological data are lacking, and consequently feasibility studies and actual designs of flood-related projects are being made based solely on the well-known Hershfield's statistical method that provides a single value for the PMP. Thus, a method to quantify the uncertainty of the PMP if Hershfield's method is to be applied has been included in this chapter.

Regardless of the method used for estimating the PMP and PMF, the current concern of climate change brings the issue on how possible changes in hydrometeorological variables such as air temperature, wind, humidity, snow cover, and sea levels may affect the estimates of extreme events in general and PMP and PMF in particular. Many studies have been made documenting possible trends in extreme precipitation and flood events and the possibility of using the so-called global climate model (GCM) outputs and projections for estimating extreme events, but results are still debatable and controversial (e.g., [25,46,65]). A review on efforts made on this issue in the past decades is available [25].

Acknowledgments

We acknowledge the cooperation received from Ings. Alvaro Prada Arciniegas (Metropolitan Aqueduct of Bucaramanga), Jairo Jaramillo Vallejos (Conalvias S. A.), and Juan Luis Cadavid (Integral Consulting Engineers, Colombia), in connection with the study of the Tona River dam at Bucaramanga, Colombia, which was quite useful in writing this chapter. Also acknowledgment is due to Dr. John F. England of the USBR for providing us with useful material for preparing this chapter.

References

1. Alexander, G.N. 1963. Using the probability of storm transposition for estimating the frequency of rare floods. *J. Hydrol.* 1, 46–57.
2. AT (Alberta Transportation). 2004. Guidelines on extreme flood analysis, Transportation & Civil Engineering Division, Civil Projects Branch, 87 pages + Appendices, Alberta, Canada.
3. Barker, B., Schaefer, M.G., Mumford, J., and Swain, R. 1997. A Monte Carlo approach to determine the variability of PMF estimates, Final Report on Bumping Lake Dam for USBR Dam Safety Office.

4. Benson, M.A. 1973. Thoughts on the design of design floods. Floods and droughts, *Proceedings of the 2nd International Symposium in Hydrology*, Fort Collins, CO, Water Resources Publications, pp. 27–33.
5. BIDR-WE (China Water Resources Beifang Investigation Design and Research Co. Ltd. and China International Water & Electric Corporation). 2009. Kohala Hydropower Project, Updating of Feasibility Study, Main Report, Chapter 3, Hydrology.
6. Bondelid, T.R., McCuen, R.H., and Jackson, T.J. 1982. Sensitivity of SCS models to curve number variation. *Water Res. Bull*. 18(1), 111–116.
7. Botero, B.A. and Frances, F. 2010. Estimation of high return period flood quantiles using additional non-systematic information with upper bounded statistical models. *Hydrol. Earth Syst. Sci*. 14, 2617–2628, EGU.
8. Casas, C.M., Rodríguez, R., Nieto, R., and Redaño, A. 2008. The estimation of probable maximum precipitation, the case of Catalonia. *Ann. N. Y. Acad. Sci*. 1146, 291–302.
9. Chow, V.T. 1951. A general formula for hydrologic frequency analysis. *Trans. Am. Geophys. Union* 32, 231–237.
10. Chow, V.T., Maidment, D.R., and Mays, L.W. 1988. *Applied Hydrology*, McGraw Hill Book, Co., New York.
11. Cohn, T.A., Lane, W.L., and Baier, W.G. 1997. An algorithm for computing moments-based flood quantile estimates when historical information is available. *Water Resour. Res*. 33(9), 2089–2096.
12. Collier, C.G. and Hardaker, P.J. 1996. Estimating probable maximum precipitation using a storm model approach. *J. Hydrol*. 183, 277–306.
13. Cotton, W.R., McAnelly, R.A., and Ashby, T. 2003. Development of new methodologies for determining extreme rainfall, Department of Atmospheric Sciences, Colorado State University, Fort Collins, CO.
14. Cudworth, A.G. 1989. *Flood Hydrology Manual*, A Water Resources Technical Publication, Bureau of Reclamation, Denver, CO, 243pp.
15. Dawdy, D.R. and Lettenmaier, D.P. 1987. Initiative for risk-based flood design. *ASCE J. Hydrau. Eng*. 113(8), 1041–1051.
16. Desa, M.N. and Rakhecha, P.R. 2007. Probable maximum precipitation for 24-hr duration over an equatorial region: Part 2-Johor. Malaysia. *Atmos. Res*. 84, 84–90.
17. Dhar, O.N., Kulkarni, A.K., and Rakhecha, P.R. 1980. Probable maximum point rainfall estimation for the southern half of the Indian peninsula. *Proc. Indian Acad. Sci. (Earth Planet. Sci.)* 90(1), 39–46.
18. DID (Department of Irrigation and Drainage). 2000. *Urban Stormwater Management Manual (MSMA Manual)*, Percetakan Nasional Malaysia, Kuala Lumpur, Malaysia, p. 13-3.
19. Douglas, E.M. and Barros, A.P. 2003. Probable maximum precipitation estimation using multifractals: Application in the eastern United States. *J. Hydrometeorol*. 4, 1012–1024.
20. Dwyer, I.J. and Reed, D.W. 1994. Effective fractal dimension and corrections to the mean of annual maxima. *J. Hydrol*. 157, 13–34.
21. England, J.F., Jarrett, R.D., and Salas, J.D. 2003. Comparisons of two moment-based estimators that utilize historical and paleoflood data for the log-Pearson type III distribution. *Water Resour. Res*. 39(9), 1243, doi:10.1029/2002WR001791.
22. England, J.F. 2006. Frequency analysis and two-dimensional simulations of extreme floods on a large watershed. PhD dissertation, Department of Civil and Environmental Engineering, Colorado State University, Fort Collins, CO.
23. England, J.F., Velleux, M.L., and Julien, P.Y. 2007. Two-dimensional simulations of extreme floods on a large watershed. *J. Hydrol*. 347(1–2), 229–241.
24. England, J.F. 2011. Flood frequency and design flood estimation procedures in the United States: Progress and challenges. *Aust. J. Water Resour*. 15(1), 33–46.

25. England, J.F., Sankovich, V.L., and Caldwell, R.J. December 2011. Review of probable maximum precipitation procedures and databases used to develop hydrometeorological reports, U.S.B.R., Report for the Nuclear Regulatory Commission.
26. Fontaine, T.A. and Potter, K.W. 1989. Estimating probabilities of extreme rainfalls, *ASCE J. Hydrau. Eng*. 115(11), 1562–1575.
27. Foufoula-Georgiou, E. 1989. A probabilistic storm transposition approach for estimating exceedance probabilities of extreme precipitation depths, *Water Resour. Res*. 25(5), 799–815.
28. Frances, F., Salas, J.D., and Boes, D.C. (1994). Flood frequency analysis with systematic and historical or paleoflood data based on the two-parameter general extreme value models, *Water Resour. Res*. 30(5), 1653–1664.
29. Grimaldi, S., Petroselli, A., Tauro, F., and Porfiri, M. 2012. Time of concentration: A paradox in modern hydrology, *Hydrol. Sci. J*. 57(2), 217–228.
30. Gupta, V.K. 1972. Transposition of storms for estimating flood probability distributions, Hydrology Papers 59, Colorado State University, Fort Collins, CO.
31. Hansen, E.M., Schreiner, L.C., and Miller, J.F. 1982. Application of probable maximum precipitation estimates—United States East of 105th Meridian, Hydrometeorological Report 52, US Department of Commerce, NOAA, US Weather Bureau, Washington, DC.
32. Hansen, E.M. 1987. Probable maximum precipitation for design floods in the United States, *J. Hydrol*. 96, 267–278.
33. Hansen, E.M., Fenn, D.D., Schreiner, L.C., Stodt, R.W., and Miller, J.F. 1988. Probable maximum precipitation estimates—United States between the Continental Divide and the 103rd Meridian, Hydrometeorological Report 55A, National Weather Service, NOAA, US Department of Commerce, Silver Spring, MD, 168p.
34. Harris, J. and Brunner, G. 2011. Approximating the probability of the probable maximum flood, *Proceedings of the World Environmental and Water Resources Congress*, *ASCE*, Palin Springs, California, pp. 3695–3702.
35. Hershfield, D.M. 1961. Estimating the probable maximum precipitation, *ASCE J. Hydrau. Div*. 87(5), 99–116.
36. Hershfield, D.M. 1965. Method for estimating probable maximum rainfall, *J. AWWA* 57, 965–972.
37. Ho, F.P. and Riedel, J.T. 1980. Seasonal variation of 10-square-mile probable maximum precipitation estimates, United States East of the 105th Meridian, Hydrometeorological Report 53, National Weather Service, NOAA, US Department of Commerce, Silver Spring, MD, 168p.
38. Jennings, A.H. 1950. World's greatest observed point rainfalls. Hydrometeorological Section, US Weather Bureau, Washington, DC, pp. 4–5.
39. Johnson, B.E., Julien, P.Y., Molnár, D.K., and Watson, C.C. 2000. The two-dimensional upland erosion model CASC2D-SED, *J. Am. Water Resour. Assoc*. 36(1), 31–42.
40. Julien, P.Y., Saghafian, B., and Ogden, F.L. 1995. Raster-based hydrologic modeling of spatially-varied surface runoff. *Water Resour. Bull., AWRA* 31(3), 523–536
41. Julien, P.Y. and Rojas, R. 2002. Upland erosion modeling with CASC2D-SED, *Int. J. Sediment Res*. 17(4), 265–274.
42. Kendall, M. and Stuart, A. 1963. *The Advanced Theory of Statistics*, Vol. 1, *Distribution Theory*, 2nd edn., Hafner Publishing Company, Inc., New York.
43. Klemes, V., Nikleva, S., and Chin, W.Q. 1992. Probability of a PMP—A feasibility study. *Dam Safety* 1992, 1–16.
44. Klemes, V. 1993. Probability of extreme hydrometeorological events—A different approach. *Proceedings of the Yokohama Symposium*, July, IAHS Pub. No. 213, pp. 167–176.
45. Koutsoyiannis, D. 1999. A probabilistic view of Hershfield's method for estimating probable maximum precipitation. *Water Resour. Res*. 35(4), 1313–1322.
46. Kundzewicz, Z.W. and Stakhiv, E. 2010. Are climate models "ready for prime time" in water resources management applications, or is more research needed? *Hydrol. Sci. J*. 55(7), 1085–1089.

47. Laurenson, E.M. and Kuczera, G.A. 1999. Annual exceedance probability of probable maximum precipitation. *Aust. J. Water Resour*. 3(2), 167–176.
48. Loukas, A. and Quick, M.C. 1996. Physically-based estimation of lag time for forested mountainous watersheds. *Hydrol. Sci. J*. 41(1), 1–19.
49. McCuen, R.H. 2009. Uncertainty analyses of watershed time parameters. *ASCE J. Hydrol. Eng*. 14(5), 490–498.
50. Mejia, G. and Villegas, F. 1979. Maximum precipitation deviations in Colombia. *Third Conference on Hydrometeorology*, *American Meteorological Society*, Boston, MA, pp. 74–76, August 20–24, Bogota, Colombia.
51. Merz, B. and Thieken, A.H. 2005. Separating natural and epistemic uncertainty in flood frequency analysis, *J. Hydrol*. 309, 114–132.
52. Mood, A., Graybill, F., and Boes, D.C. 1974. *Introduction to the Theory of Statistics*, 3rd edn., McGraw Hill, New York.
53. Nathan, R.J. and Weinmann, P.E. 2001. Estimation of large to extreme floods, Book VI in *Australian Rainfall and Runoff: A Guide to Flood Estimation*, National Committee on Water Engineering, Institution of Engineers, Australia.
54. Nathan, R.J. and Merz, S.K. November 2001. Estimation of extreme hydrologic events in Australia: Current practice and research needs. *Proceedings of the Hydrologic Research Needs for Dam Safety*, Meeting Sponsored by FEMA, Paper 13, pp. 69–77.
55. Newton, D.W. 1983. Realistic assessment of maximum flood potentials. *ASCE J. Hydrau. Eng*. 109(6), 905–918.
56. Nobilis, F., Haiden, T., and Kerschbaum, M. 1991. Statistical considerations concerning probable maximum precipitation (PMP) in the Alpine Country of Austria. *Theor. Appl. Climatol*. 44, 89–94.
57. NRC (National Research Council). 1988. *Estimating Probabilities of Extreme Floods*, National Academy Press, Washington, DC.
58. NRC (National Research Council), 2000. *Risk Analysis and Uncertainty in Flood Damage Reduction Studies*, National Academy Press, Washington, DC, 202 pp.
59. NWS (National Weather Service). 1980. Probable maximum precipitation estimates, United States between the Continental Divide and the 103rd Meridian. Hydrometeorological Report 55A, Silver Spring, MD, 259pp.
60. NWS (National Weather Service). October 1994. Probable maximum precipitation for the Pacific Northwest States—Columbia, Snake River, and Pacific Coastal Drainages, Hydrometeorological Report 57, Silver Spring, MD.
61. O'Connell, D.R.H., Ostenaa, D.A., Levish, D.R., and Klinger, R.E. 2002. Bayesian flood frequency analysis with paleoflood bound data. *Water Resour. Res*. 38(5), 14, DOI 10.1029/2000WR000028.
62. Ohara, N., Kavvas, M.L., Kure, S., Chen, Z.Q., Jang, S., and Tan, E. 2011. Physically based estimation of maximum precipitation over the American River Watershed, California. *ASCE J. Hydrol. Eng*. 16(4), 351–361.
63. Papalexiou, S.M. and Koutsoyiannis, D. 2006. A probabilistic approach to the concept of probable maximum precipitation. *Adv. Geosci*. 7, 51–54.
64. Poon, H.C. and Hwee, H.H. 2010. Probable maximum precipitation derivation in Malaysia: review and comparison. *Int. J. Hydro-Climatic Eng*. 1(ii) 37–72.
65. Prasad, R., Hibler, L.F., Coleman, A.M., and Ward, D.L. 2011. Design-basis flood estimation for site characterization at nuclear power plants in the United States of America, NUREG/CR-7046, PNNL-20091, Office of Nuclear Regulatory Research, Pacific Northwest National Laboratory, Richland, WA.
66. Rakhecha, P.R. and Soman, M.K. 1994. Estimation of probable maximum precipitation for a 2-day duration: Part 2—North Indian region. *Theor. Appl. Climatol*. 49, 77–84.
67. Receanu, R., Hertig, J.A., and Fallot, J.M., 2012. The estimation of PMP and PMF on Alpine basins in Switzerland. *Aerul si Apa: Componente ale Mediului,* Cluj University Press, 212–219.

68. Rezacova, D., Pesice, P., and Sokol, Z. 2005. An estimation of the probable maximum precipitation for river basins in the Czech Republic. *Atmos. Res*. 77, 407–421.
69. Riedel, J.T. and Schreiner, L.C. 1980. Comparison of generalized estimates of probable maximum precipitation with greatest observed rainfalls, Tech. Report NWS No. 25, National Weather Service, US Department of Commerce, Silver Spring, MD, 66pp.
70. Smith, J.B., Barker, B.L., and Pernela, L.M. 2010. Annual exceedance probability of probable maximum flood using a stochastic hydrologic model, *Proceedings of the 30th Annual USSD Conference: Collaborative Management of Integrated Watersheds*, Sacramento, CA, April 12–16, 2010. CD-ROM.
71. Stedinger, J.R. and Cohn, T.A. 1986. Flood frequency analysis with historical and paleoflood information, *Water Resour. Res*. 22(8), 785–793.
72. Stedinger, J.R., Vogel, R.M., and Foufoula-Georgiou, E. 1993. Frequency analysis of extreme events, in *Handbook of Hydrology* (D.R. Maidment, Ed.), Chapter 18, McGraw Hill, New York.
73. Swain, R.E., England, J.F., Bullard, K.L., and Raff, D.A. June 2006. *Guidelines for Evaluating Hydrologic Hazards*, US Department of the Interior, Bureau of Reclamation.
74. Thomas, W.O. Jr., Monde, M.C., and Davis, S.R., 2000. Estimation of time of concentration for Maryland streams, Transportation Research Record 1720, Paper No. CO-1267, pp. 95–99.
75. USACE (US Army Corps of Engineers). 1990. HEC-1 hydrograph package, Hydrologic Engineering Center, Davis, CA.
76. USACE (US Army Corps of Engineers). 2010. *Hydrologic Modeling System HEC-HMS—User's Manual*, August 2010, USACE, Davis, CA.
77. USBR (US Bureau of Reclamation). 1999. A framework for characterizing extreme floods for dam safety risk assessment, prepared by Utah State University and USBR, Denver, CO, 67pp.
78. USBR (US Bureau of Reclamation). 2002. Hydrologic risk analysis and extreme flood considerations, Interim Guidance for Bureau of Reclamation Dam Safety Office, D-6600, July, 3pp.
79. Velleux, M.L. 2005. Spatially distributed model to assess watershed contaminant transport and fate, PhD dissertation, Department of Civil and Environmental Engineering, Colorado State University, Fort Collins, CO.
80. Velleux, M.L., Julien, P.Y., Rojas-Sanchez, R., Clements, W., and England, J.F. 2006. Simulation of metals transport and toxicity at a mine-impacted watershed: California Gulch, Colorado. *Environ. Sci. Technol.* 40(22), 6996–7004
81. Wang, B.H. 1984. Estimation of probable maximum precipitation: Case studies. *ASCE J. Hydrau. Eng*. 110(10), 1457–1472.
82. WMO (World Meteorological Organization). 1973. Manual for estimation of probable maximum precipitation. Operational Hydrology Report 1, 1st edn., Publication 332, WMO, Geneva, Switzerland.
83. WMO (World Meteorological Organization). 1986. Manual for estimation of probable maximum precipitation. Operational Hydrology Report 1, 2nd edn., Publication 332, WMO, Geneva, Switzerland.
84. WMO (World Meteorological Organization). 2009. Manual on estimation of probable maximum precipitation (PMP), WMO-No. 1045, 259 pp.